scientific reports

Check for updates

OPEN

Methadone directly impairs central nervous system cells in vitro

Cristian De Gregorio[1,8], Javiera Gallardo[2,8], Pablo Berríos-Cárcamo[2,8], Álex Handy[3], Daniela Santapau[2], Antonia González-Madrid[2], Marcelo Ezquer[2], Paola Morales[4], Alejandro Luarte[5,6], Daniela Corvalán[5,6], Úrsula Wyneken[5,6] & Fernando Ezquer[2,7]✉

Methadone is a synthetic long-acting opioid that is increasingly used in the replacement therapy of opioid-addicted patients, including pregnant women. However, methadone therapy in this population poses challenges, as it induces cognitive and behavioral impairments in infants exposed to this opioid during prenatal development. In animal models, prenatal methadone exposure results in detrimental consequences to the central nervous system, such as: (i) increased neuronal apoptosis; (ii) disruption of oligodendrocyte maturation and increased apoptosis and (iii) increased microglia and astrocyte activation. However, it remains unclear whether these deleterious effects result from a direct effect of methadone on brain cells. Therefore, our goal was to uncover the impact of methadone on single brain cell types in vitro. Primary cultures of rat neurons, oligodendrocytes, microglia, and astrocytes were treated for three days with 10 µM methadone to emulate a chronic administration. Apoptotic neurons were identified by cleaved caspase-3 detection, and synaptic density was assessed by the juxtaposition of presynaptic and postsynaptic markers. Apoptosis of oligodendrocyte precursors was determined by cleaved caspase-3 detection. Oligodendrocyte myelination was assessed by immunofluorescence, while microglia and astrocyte proinflammatory activation were assessed by both immunofluorescence and RT-qPCR. Methadone treatment increased neuronal apoptosis and reduced synaptic density. Furthermore, it led to increased oligodendrocyte apoptosis and a reduction in the myelinating capacity of these cells, and promoted the proinflammatory activation of microglia and astrocytes. We showed that methadone, the most widely used drug in opioid replacement therapy for pregnant women with opioid addiction, directly impairs brain cells in vitro, highlighting the need for developing alternative therapies to address opioid addiction in this population.

Keywords Methadone, Neurodegeneration, Opioid addiction, Brain damage, Neuroinflammation, Opioid substitution therapy

Opioid Use Disorder (OUD) is a medical condition characterized by problematic and uncontrolled use of opioids, commonly prescribed for relieving acute and chronic pain. Beyond their potent analgesic effects, opioid consumption induces a profound sense of euphoria and well-being, making them highly addictive substances[1]. According to the United Nations World Drug Report 2020, over 19.4 million people worldwide suffer from OUD, resulting in more than 120,000 annual deaths, constituting two-thirds of all drug overdose fatalities[2]. Furthermore, in the United States and Europe, opioids are considered the most problematic drugs, driving 60% of the total demands for drug treatment[3,4]. This concerning trend is also emerging in South America countries, representing a severe issue with profound economic, social and public health consequences[2].

Globally, one-third of individuals with OUD are women, and 80% of them are in the reproductive age[5]. Consequently, the incidence of newborns delivered by mothers addicted to opioids has quadrupled over the last decade in the United States, accounting for 5 per 1000 live births[6], with 7% of routine maternal testing showing positive for opioids at the time of delivery[7]. Currently, the only therapy approved by the United States Food and

[1]Department of Biology, Università degli Studi di Padova, Padua, Italy. [2]Center for Regenerative Medicine, Faculty of Medicine, Clínica Alemana-Universidad del Desarrollo, Avenida Plaza 680, Santiago, Chile. [3]Faculty of Natural Sciences, Mathematics, and Environment, Universidad Tecnológica Metropolitana, Santiago, Chile. [4]Program of Molecular and Clinical Pharmacology, ICBM, Department of Neuroscience, Faculty of Medicine, Universidad de Chile, Santiago, Chile. [5]Neuroscience Program, Centro de Investigación e Innovación Biomédica (CiiB), Universidad de los Andes, Santiago, Chile. [6]IMPACT, Center of Interventional Medicine for Precision and Advanced Cellular Therapy, Santiago, Chile. [7]Research Center for the Development of Novel Therapeutics Alternatives for Alcohol Use Disorders, Santiago, Chile. [8]These authors contributed equally: Cristian De Gregorio, Javiera Gallardo and Pablo Berríos-Cárcamo. ✉email: eezquer@udd.cl

Drug Administration (FDA) for treating OUD, including pregnant women with OUD, involves replacing the abused short-acting opioid, such as fentanyl, morphine, or heroin, with a safer, long-acting synthetic opioid, such as methadone, administered under medical supervision. The final goal of this Opioid Replacement Therapy (ORT) is to avoid the harmful effects of opioid withdrawal symptoms and mitigate risky behaviors associated with relapse or overdose[8]. Indeed, opioid abstinence in pregnant women with OUD is strongly discouraged due to elevated risk associated with detoxification during pregnancy, including high rates of relapse, overdose death, and extreme maternal stress, potentially harming the fetus[9–11]. However, this replacement therapy also presents significant challenges because methadone readily crosses the placenta, resulting in short- and long-term alterations in the developing brain prenatally exposed to this opioid[12–14].

Several reports have indicated that children exposed to methadone during prenatal development face an elevated risk of experiencing both acute and long-term neurodevelopmental impairments. Infants between one and three months of age who have experienced in utero exposure to methadone exhibited white matter lesions, congenital structural malformations, and reduced brain volume[15]. In a later stage of development (2-year-old), these infants showed lower scores in motor and cognitive tests, including impairment in linguistic skills[16]. Additionally, they demonstrated poor regulation in crucial aspects such as self-control, emotions, feeding, learning, memory and sensory processing[16,17], which may be directly correlated with reduced brain volume and neuronal death compared to infants not exposed to methadone[18]. In fact, prenatal exposure to methadone has been linked to lower cognitive scores, reduced learning capacity, impaired short- and long-term memory, and increased anxiety in later developmental stages[16,17,19,20].

Several of the cognitive and behavioral alterations previously mentioned have also been observed in animal models of in utero methadone exposure. For example, young rats prenatally exposed to methadone exhibit deficits in cognitive function, with a decrease in spatial learning and recognition memory compared to control animals[21]. Similarly, exposure to methadone during gestation and lactation significantly increased anxiety in juvenile rats[22]. In these animal models, researchers have also evaluated the effects of methadone on central nervous system (CNS) cells, including neurons, oligodendrocytes, microglia and astrocytes.

At the cellular level, structural and functional alterations identified in the brains of animals exposed to methadone in utero include: (i) increased neuronal apoptosis and reduced neurogenesis[23]; (ii) disruption of the maturation and induction of apoptosis of oligodendrocytes, responsible for producing myelin that surrounds neuronal axons, resulting in altered myelination[24]; and (iii) proinflammatory activation of microglia and astrocytes, the immune cells of the CNS, in specific brain regions including the hippocampus and prefrontal cortex[25]. These cellular alterations are considered key contributors to the cognitive and behavioral impairments commonly observed in animal models exposed to methadone *in utero*[25,26].

Despite these findings in the brain of animals prenatally exposed to methadone, the understanding of whether these impairments result from methadone-induced signaling cascades over different neural cell types, instead of a consequence of secondary insults of methadone toxicity, remain to be studied. To explore these aspects, we utilized highly enriched primary cultures of rat neurons, oligodendrocytes, microglia, and astrocytes during the mid-to-late period of brain development. Each cell type was treated individually with methadone for three days to mimic the chronic methadone exposure of fetal brain cells in the opioid replacement therapy for pregnant women. Under this methadone exposure paradigm, we assessed the direct impact of this drug on cell survival and cell function. Data indicated that methadone exposure significantly alters the survival and functionality of isolated cells, suggesting that new therapies to reduce methadone brain ailments would need to address neuron, oligodendrocytes, microglia, and astrocyte toxicity, emphasizing the importance of finding new non-opioid based pharmacotherapies for OUD in pregnant women.

Results

To explore the autonomous cellular effects of methadone on different neural cell types during brain development, we established highly enriched primary cell cultures. Neurons were obtained from the brain of rat embryos at embryonic day 18 (E18), while astrocytes, microglia and oligodendrocytes were purified from the brain of rats at postnatal day 0 (P0). Immunofluorescence analysis, utilizing well-established molecular markers, revealed purities ranging from 88 to 97% in each of these primary cultures (Supplementary Fig. 1).

Previous research has reported that plasma concentration of methadone in pregnant women undergoing opioid replacement therapy falls within the range of 1–2 μM[27,28]. However, the degree of methadone exposure of fetal brain cells might be higher than the observed in plasma as methadone levels have been shown to be significantly increased in the fetal brain compared to the mother brain in a rat model of prenatal methadone exposure[29], suggesting specific fetal brain accumulation. Furthermore, in vitro studies using either primary cultures or cell lines derived from human or rodents, have employed a broad range of methadone concentrations from 0.1 to 100 μM[30–32]. Thus, there is a notable gap in the literature regarding the dose that is relevant for methadone exposure on primary cultures of neurons, oligodendrocytes, microglia, and astrocytes. Therefore, we first studied the dose–response effects of methadone on cell viability in brain-derived primary cultures, conducting CellTiter-Blue assays. Neurons, oligodendrocytes, microglia, and astrocytes were incubated for three days with increasing concentrations of methadone to determine the concentration were cell viability is inhibited by 50% (IC_{50}) for each cell type. Intriguingly, all IC_{50} values consistently fell within the same concentration range (20–50 μM), Fig. 1, close to the physiologically relevant concentration discussed above, suggesting that methadone effectively induces an autonomous-cellular toxic response. Based on these results, we opted for a 10 μM methadone dose, which is below the IC_{50} for all cell types, to assess the functional and morphological responses of each cell type after three days of methadone exposure, aiming to emulate a chronic methadone exposure scenario for fetal brain cells during opioid substitution therapy in pregnant women.

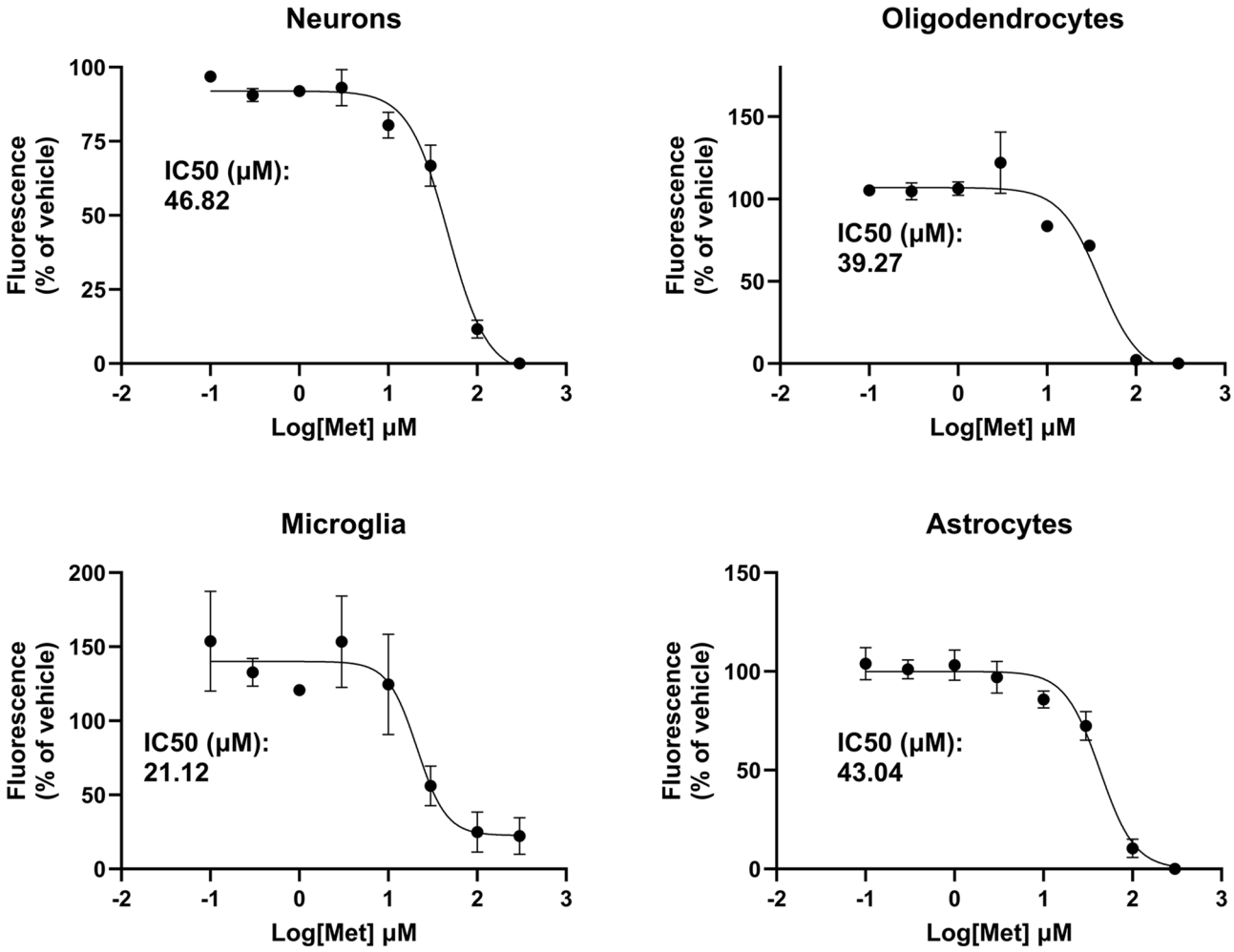

Figure 1. Methadone-induced IC_{50} in highly purified cortex-derived primary cells cultures. Different cell type cultures from the CNS were subjected to increasing methadone concentration (ranging from 0.3 to 300 μM) for three days, and cell viability was assessed using CellTiter-Blue analysis. Fluorescence plots illustrate the dose–response impact of methadone on cell viability in neurons (**A**), oligodendrocytes (**B**), astrocytes (**C**), and microglia (**D**) cultures. The IC_{50} values for each cell type were determined adjusting the data to a non-linear equation of methadone concentration vs. normalized response. Plots display the mean fluorescence ± SEM. Assays were conducted with 3 different biological replicates with 6 technical replicates each.

Methadone triggers neuronal apoptosis and reduces synaptic density in primary neurons in vitro

Previous studies have shown that opioid exposure, including methadone, significantly decreases the number of mature neurons in the hippocampus and prefrontal cortex in vivo[33,34], and impair synaptic transmission in cortical organoids in vitro[35]. To investigate the direct impact of methadone treatment on neuronal viability and synaptic structure establishment, we modeled a chronic methadone exposure (three days in vitro) using rat primary cortical neurons. Data showed that methadone treatment increased the levels of cleaved caspase-3 (cCaspase-3), compared with vehicle-treated cells, evaluated by Western Blot, indicating a significant rise in the neuronal apoptotic population (Fig. 2A,B; Supplementary Fig. 2). We also evaluated the co-expression of cCaspase-3 and the neuronal marker βIII-tubulin by immunofluorescence. The analysis confirmed that methadone-treated neuron cultures exhibited a significant increase in neuronal apoptosis compared to vehicle-treated neurons (Fig. 2C,D).

Prior research utilizing cortical organoids has indicated that exposure to methadone may lead to impairments in synaptic transmission[31,35,36]. To thoroughly investigate methadone's influence on synaptic structure, we employed immunofluorescent staining to detect proteins localized at presynaptic and postsynaptic sites (specifically, Synaptophysin and PSD-95, respectively) in mature neurons (16 days post-culturing). In a functional synapse, these presynaptic and postsynaptic proteins are typically juxtaposed at a nanometric scale, a detail that, while not entirely resolvable via confocal microscopy, manifests as colocalizing areas or *puncta*. Our analysis revealed that neurons exposed to methadone exhibited a significant decrease in the quantity of these colocalizing *puncta*, in comparison to vehicle-treated neurons (Fig. 3A,B). Additionally, there was a marked reduction in the colocalization area between the two markers in methadone-treated neurons (Fig. 3C). Collectively, these

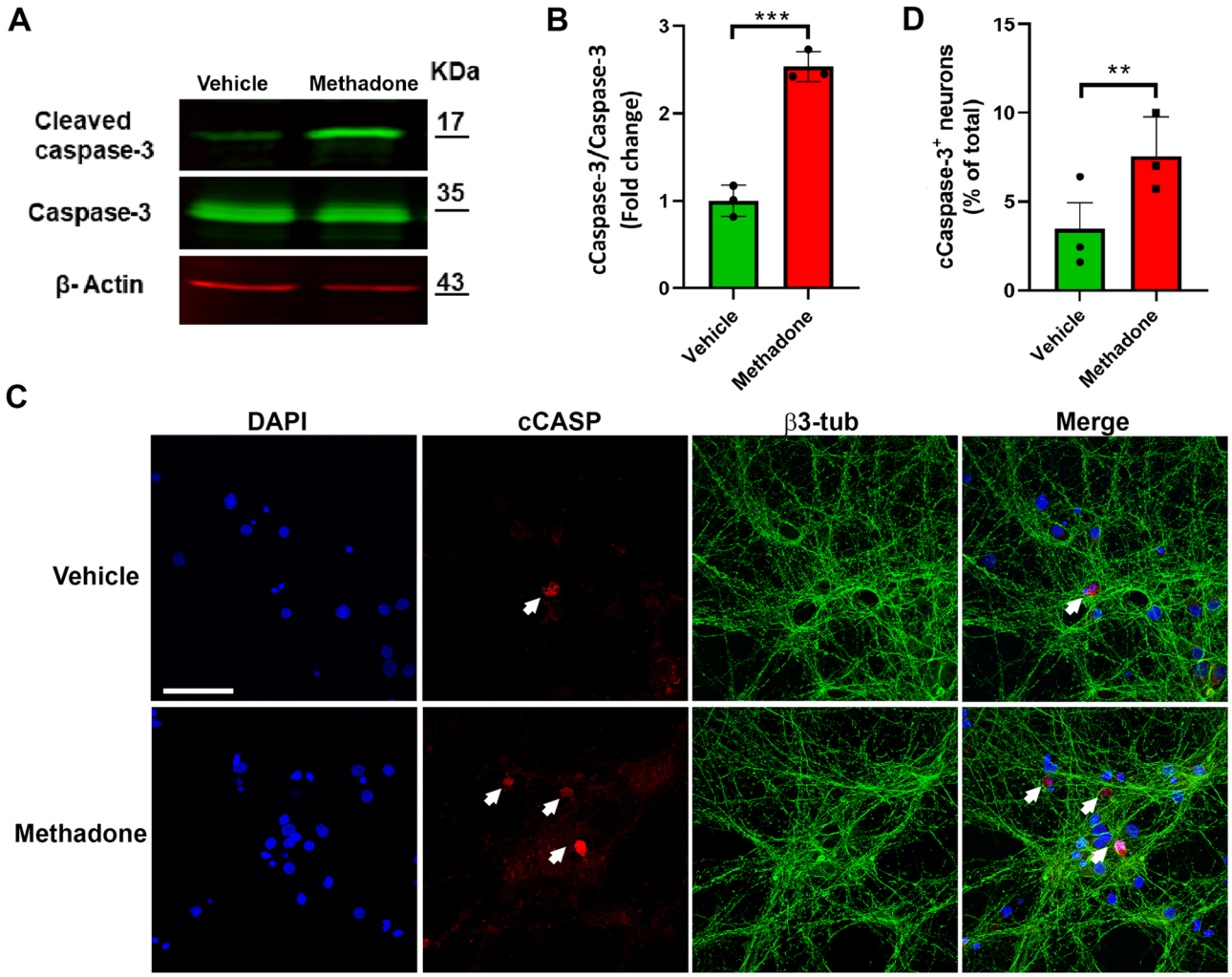

Figure 2. Chronic methadone treatment induces apoptosis of primary neurons. Six-day-old primary neuronal cultures were treated for three days with either 10 µM methadone or vehicle. (**A**) Representative Western Blot analysis showing an increased abundance of cCaspase-3 in methadone-treated neurons, with total caspase-3 and β-actin as housekeeping proteins. (**B**) Densitometric analysis from Western Blot in (A) expressed as fold change. Data are presented as MEAN ± SEM of three independent cultures. ***$p < 0.001$ Student's T-test. (**C**) Representative confocal microscopy images confirm co-expression of cCaspase-3 (red) with the neuronal marker βIII-tubulin (green). Nuclei were counterstained with DAPI (blue). Scale bar = 50 µm. White arrows indicate cCaspase-3$^+$/βIII-tubulin$^+$ cells. (**D**) Quantification of double-positive cells (cCaspase-3$^+$, βIII-tubulin$^+$) for the images depicted in (**C**). Data are presented as mean ± SEM of three independent cultures. In total, ~ 1200 neurons were quantified for each condition. **$p < 0.01$ Student's T-test.

findings indicate that methadone treatment correlates to an increase in neuronal apoptosis and a decrease in the total number of synaptic contacts in cortical neurons.

Methadone induces oligodendrocyte apoptosis and reduces the oligodendrocyte-myelinating population

Oligodendrocytes, responsible for producing myelin in the CNS, are susceptible to the effects of opioids, leading to increased cell apoptosis and diminished myelination capacity, which can result in cognitive impairments[24,37]. Previous studies have suggested that activated microglia, through the secretion of pro-inflammatory molecules, may impact the differentiation potential and survival of oligodendrocytes[38,39]. However, there is limited information available on whether methadone can directly affect oligodendrocytes in a cell-autonomous manner.

In our analysis, purified oligodendrocyte cultures exhibited a low level of oligodendrocyte precursors cells (OPCs, defined as NG2$^+$ cells), constituting a population of less than 5% of total Oligodendrocyte Specific Protein (OSP) positive cells (pan-oligodendrocyte marker[40]; data not shown), but were highly enriched in pre-myelinating oligodendrocytes, detected by the expression of the O4 marker[41] (Supplementary Fig. 3). Consequently, our focus was directed towards assessing whether methadone treatment exerts a direct impact on the viability of differentiated oligodendrocytes, rather than OPCs.

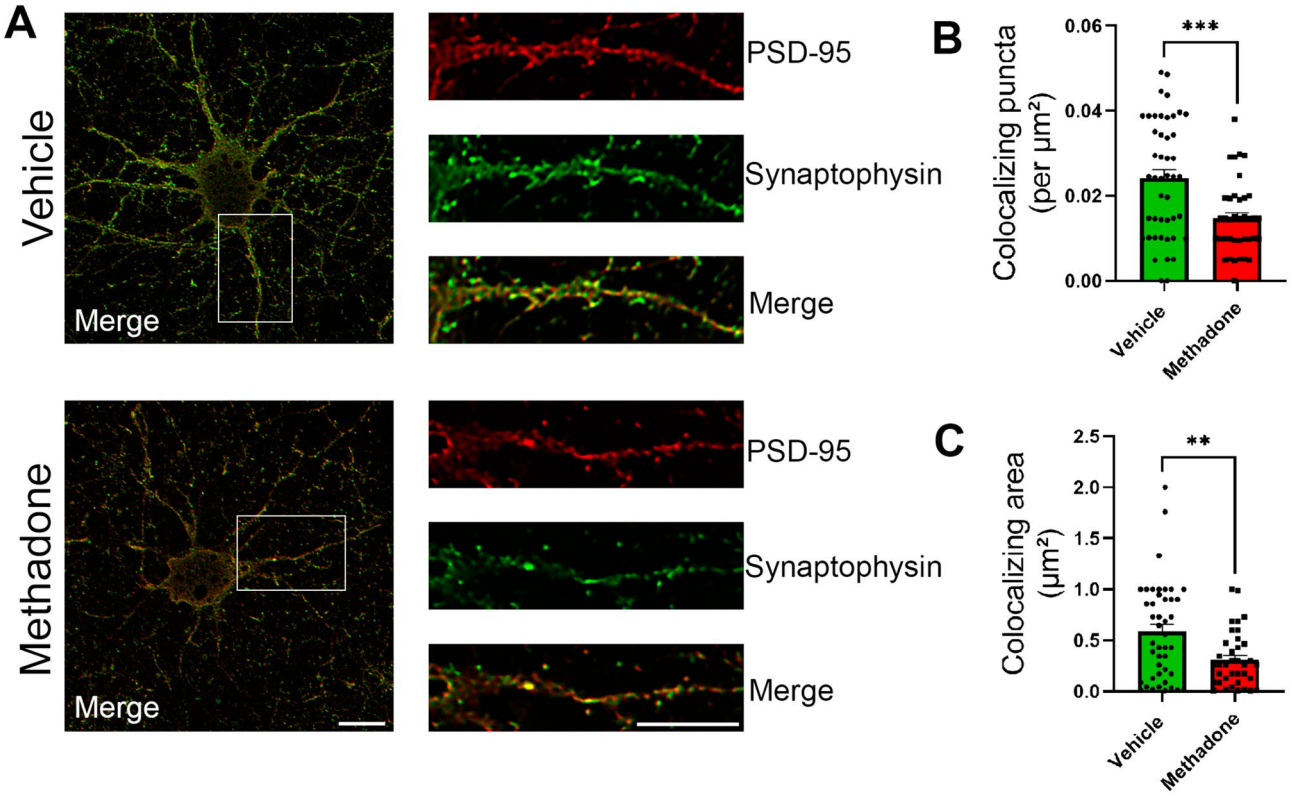

Figure 3. Chronic methadone treatment reduces synaptic density in mature primary neurons. Thirteen-day-old primary neuronal cultures were treated for three days with either 10 µM methadone or vehicle. (**A**) Representative confocal slices depict synaptic structures, revealed by the juxtaposition of a presynaptic marker puncta (synaptophysin, green) and a postsynaptic marker puncta (PSD-95, red). Scale bar = 10 µm. (**B**) Quantification of colocalizing puncta and (**C**) quantification of colocalizing area for the images depicted in (**A**). For each experimental condition, 37–48 dendritic fields were analyzed from 10 to 15 neurons. Data are presented as mean ± SEM of three independent cultures.**$p < 0.01$; ***$p < 0.001$ Mann–Whitney test.

Oligodendrocyte cultures were incubated for three days with 10 µM methadone or vehicle, and an immunofluorescence assay was performed to detect apoptotic oligodendrocytes. Data revealed a significant increase in cCaspase-3 levels in $O4^+$ oligodendrocytes following chronic methadone treatment (Fig. 4), providing evidence of increased apoptotic cell death, and underscoring the direct impact of this opioid on the viability of pre-myelinating oligodendrocytes.

Additionally, evidence supports a role of the endogenous opioid system in regulating myelination[42]. To assess whether methadone directly impairs oligodendrocyte maturation, cells were incubated for three days with either 10 µM methadone or vehicle and analyzed by immunofluorescence using different maturation markers for pre-myelinating (O4) and myelinating (MBP) stages. The changes in maturation of oligodendrocyte cultures were evaluated in the presence and absence of the thyroid hormones T3 and T4, known as maturation stimulating agents[43]. Data indicates that methadone does not alter the percentage of $O4^+$ cells (Supplementary Fig. 3); however, it significantly reduces the myelinating MBP^+ population (Fig. 5A,B). Treatment with the pro-myelinating hormones T3 and T4 results in a two-fold increase in the myelinating population in vehicle-treated oligodendrocytes (from 11.3 ± 1.1% to 22.2 ± 1.5% of total OSP^+ cells). Notably, T3/T4 hormone treatment leads to a three-fold increase in the MBP^+ population in methadone-treated oligodendrocytes (from 4.0 ± 1.1% to 13.1 ± 1.7% of total OSP^+ cells) (Fig. 5A,B, representative images of each marker in Supplementary Fig. 4). This result suggests that methadone-treated cultures may retain their maturation capacity in vitro, and methadone-induced impairments could potentially be reversed by stimulating alternative salvage pathways.

Neuroinflammatory features in methadone-treated microglia and astrocyte cultures

Given the association between chronic opioid use and the upregulation of proinflammatory cytokines at the peripheral level[44,45], as well as microglia and astrocyte activation at the brain level[46,47], we analyzed the inflammatory status in microglia and astrocytes exposed for three days to either 10 µM methadone or vehicle. An increased expression of proinflammatory markers CD11b and CD45 has been associated with microglia activation in several neuroinflammatory diseases[48]. In addition to molecular and functional changes, activated microglia undergo significant morphological transformations, with a transition from a quiescent, branched state into an amoeboid shape with retracted processes and heightened phagocytic and migratory capabilities[49,50]. Microglia activation was evaluated by immunofluorescence assay to quantify the cell population exhibiting the characteristic amoeboid

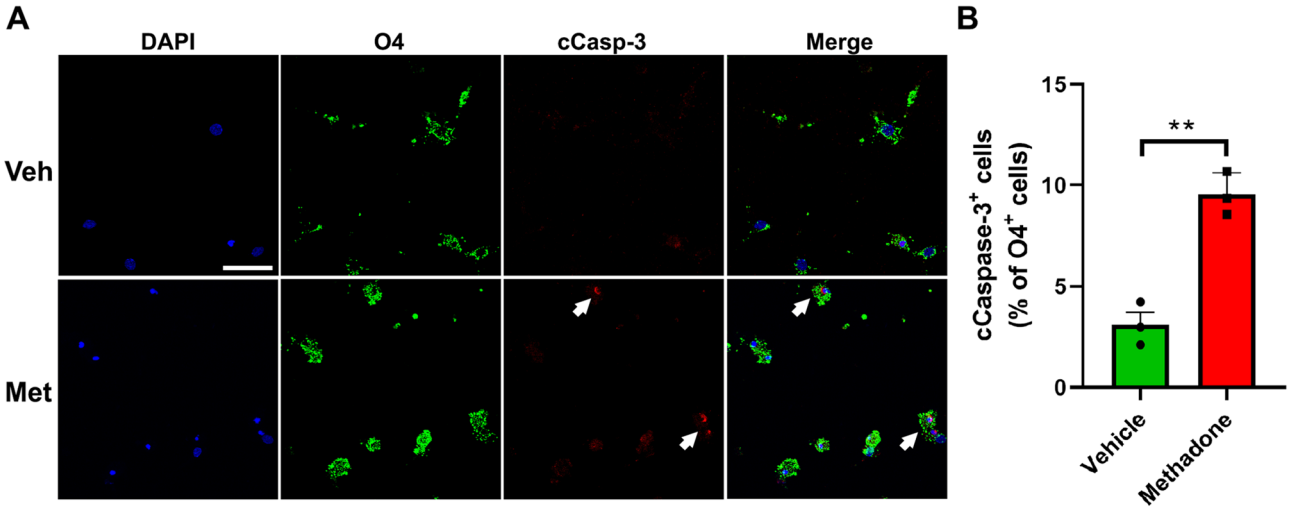

Figure 4. Chronic methadone treatment induces apoptosis of primary oligodendrocyte cells. Four-day-old primary oligodendrocyte cultures were treated for three days with either 10 µM methadone or vehicle. (**A**) Representative confocal microscopy images showing apoptotic oligodendrocytes, indicated by cCaspase-3 immunoreactivity (red). Differentiated oligodendrocytes were detected using the O4 antibody (green). Nuclei were counterstained with DAPI (blue). Scale bar = 50 µm. White arrows indicate cCasp-3$^+$ O4$^+$ cells. (**B**) Quantification of the cCaspase-3 population, expressed as a percentage of the total oligodendrocyte population (O4$^+$ cells). Data are presented as mean ± SEM of three independent cultures. In total, ~ 1000 oligodendrocytes were quantified for each condition. **p < 0.01 Student's T-test.

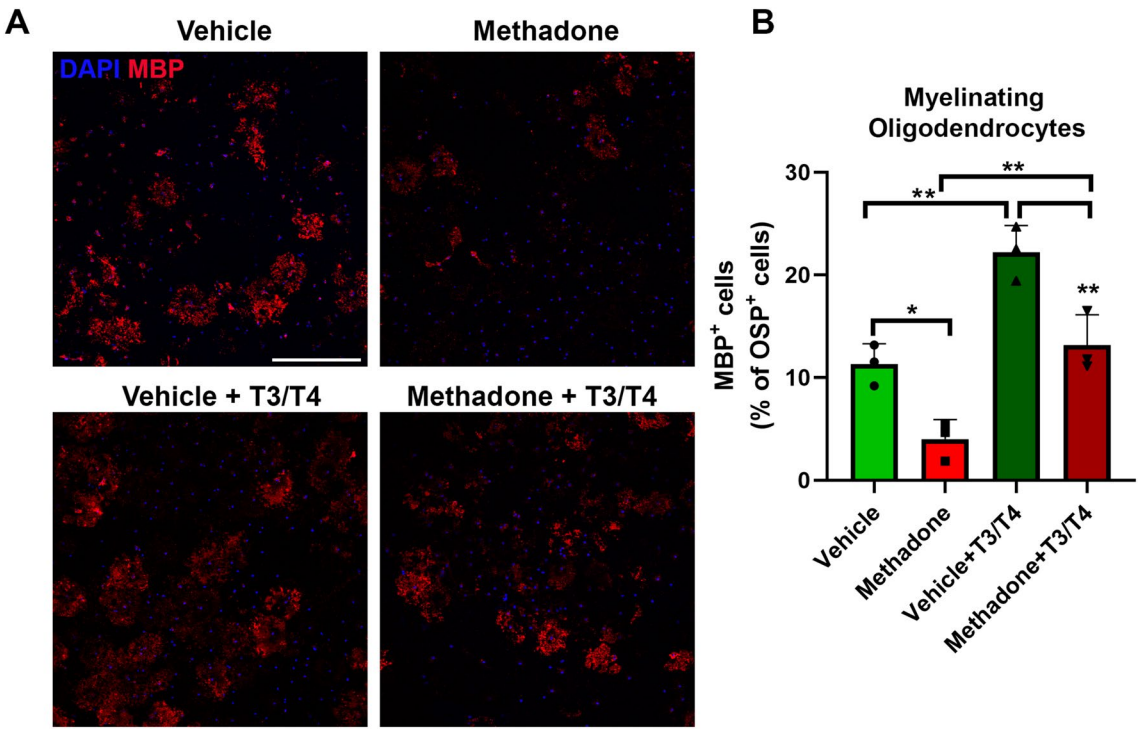

Figure 5. Chronic methadone treatment reduces the oligodendrocyte myelinating population. Four-day-old primary oligodendrocyte cultures were treated for three days with 10 µM methadone or vehicle in the presence or absence of the thyroid hormones T3 and T4 to promote myelination. (**A**) Representative confocal microscopy images showing the myelinating population, visualized through the Myelin Basic Protein marker (MBP, red). Nuclei were counterstained with DAPI (blue). Scale bar = 200 µm. (**B**) Quantification of the MBP$^+$ population, expressed as a percentage of the total oligodendrocyte population (OSP$^+$ cells, see Supplementary Fig. 4). Data are presented as mean ± SEM of three independent cultures. In total, ~ 2000 oligodendrocytes were quantified for each condition. *p < 0.05; **p < 0.01 determined by a one-way ANOVA followed by Tukey post-hoc test.

phenotype of activated microglia and elevated intensity of pro-inflammatory markers CD11b (CD11b^{high}) or CD45 (CD45^{high}), compared to the CD11b and CD45 detection in resting state microglia. Data suggests that methadone exposure effectively stimulates an inflammatory phenotype of the microglial population compared to vehicle-treated microglia (Fig. 6A–D).

Astrocytes are another key player controlling neuroinflammatory cascades[51]. Previously, using mixed glial cultures containing astrocytes and microglia, it was found that endogenous (met-enkephalin) or exogenous (morphine) opioids can induce astrocytes activation, evidenced by a transition from a hexagonal to a branched, hypertrophic shape under in vitro conditions[52–54], often influenced by the proinflammatory molecules secreted by activated microglia[55]. However, in this instance, we want to analyze whether methadone could stimulate astrocytic activation at a cell-autonomous level, using highly pure primary astrocyte cultures. Through immunofluorescence analysis, we determined that astrocyte cultures incubated for three days with 10 µM methadone exhibited an activated phenotype compared to vehicle-treated cells. This was evidenced by a significant increase in the average cell area and in the number of cellular processes per cell (Fig. 7A–C). Additionally, astrocyte activation was evaluated by quantifying GFAP^{+} cells showing high levels of the astrocyte activation marker CD38[56] through immunofluorescence. In agreement with previous morphological data, we showed that methadone treatment induced a significant increase in the number of CD38^{high} astrocytes compared to vehiche-treated cells (Fig. 7D,E). To support our results, the mRNA levels of classic proinflammatory cytokines were compared between methadone-treated microglia and astrocytes versus vehicle-treated cells by RT-qPCR. Importantly, for these experiments we supplemented microglia cultures with macrophage colony-stimulating factor (M-CSF), a

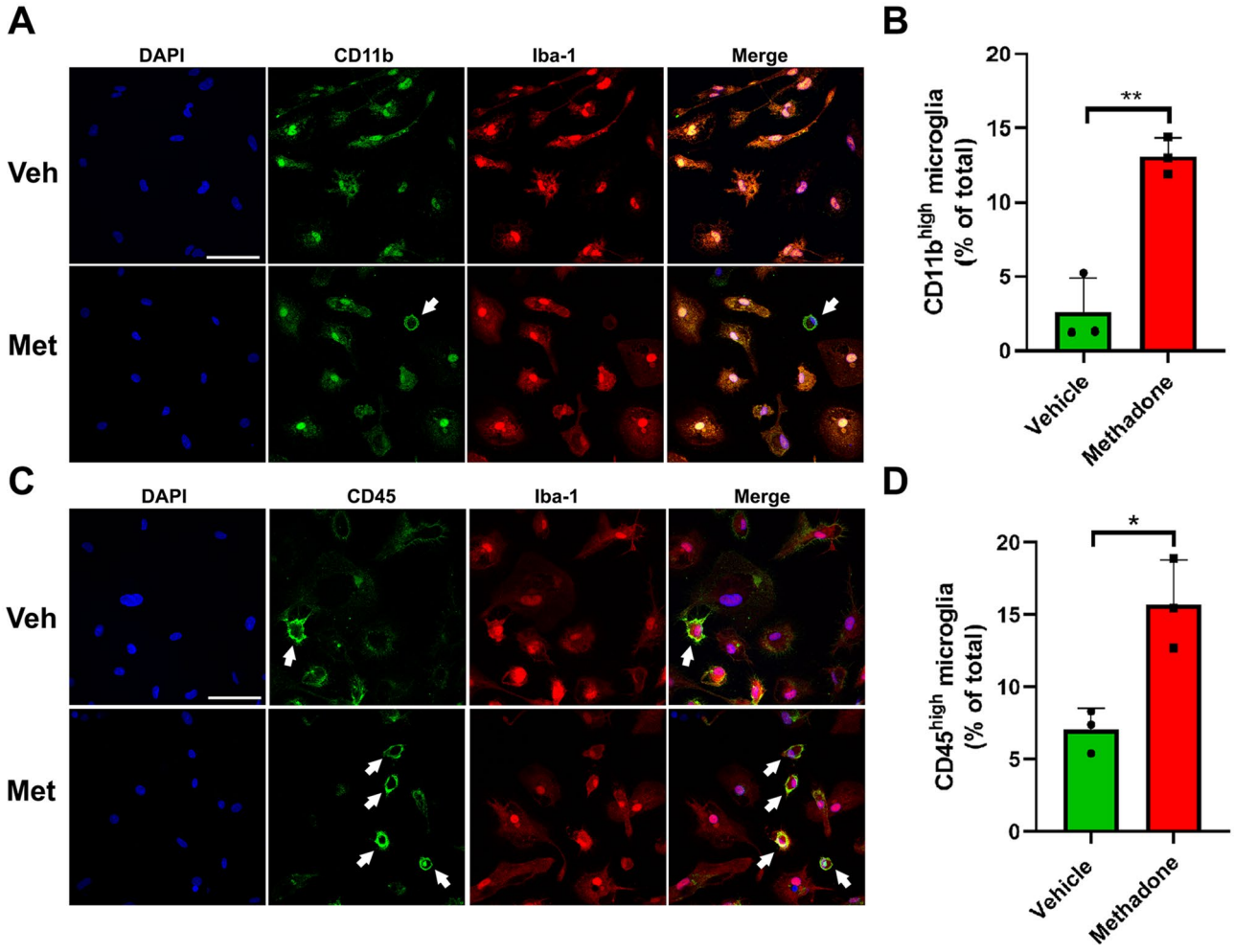

Figure 6. Chronic methadone treatment induces microglial activation. One-day-old primary microglia cultures were treated for three days with either 10 µM methadone or vehicle. (**A**, **C**) Representative confocal microscopy images illustrating microglial activation, evidenced by changes in cellular morphology and the expression of the activation-associated markers CD11b (green, **A**) and CD45 (green, **C**). Microglial cells were detected using an anti-Iba-1 antibody (red). Nuclei were counterstained with DAPI (blue). Scale bar = 50 µm. Arrows indicate the presence of microglia expressing high levels of the activation-associated markers and exhibiting an amoeboid morphology. (**B**, **D**) Quantification of activated microglia based on increased levels of the activation-associated markers (CD11b^{high}) (**B**) and CD45^{high} (**D**), combined with an amoeboid cell morphology. Data are presented as mean ± SEM of three independent cultures. In total, ~ 500 microglia were quantified for each condition. *p < 0.05; **p < 0.01 Student's T-test.

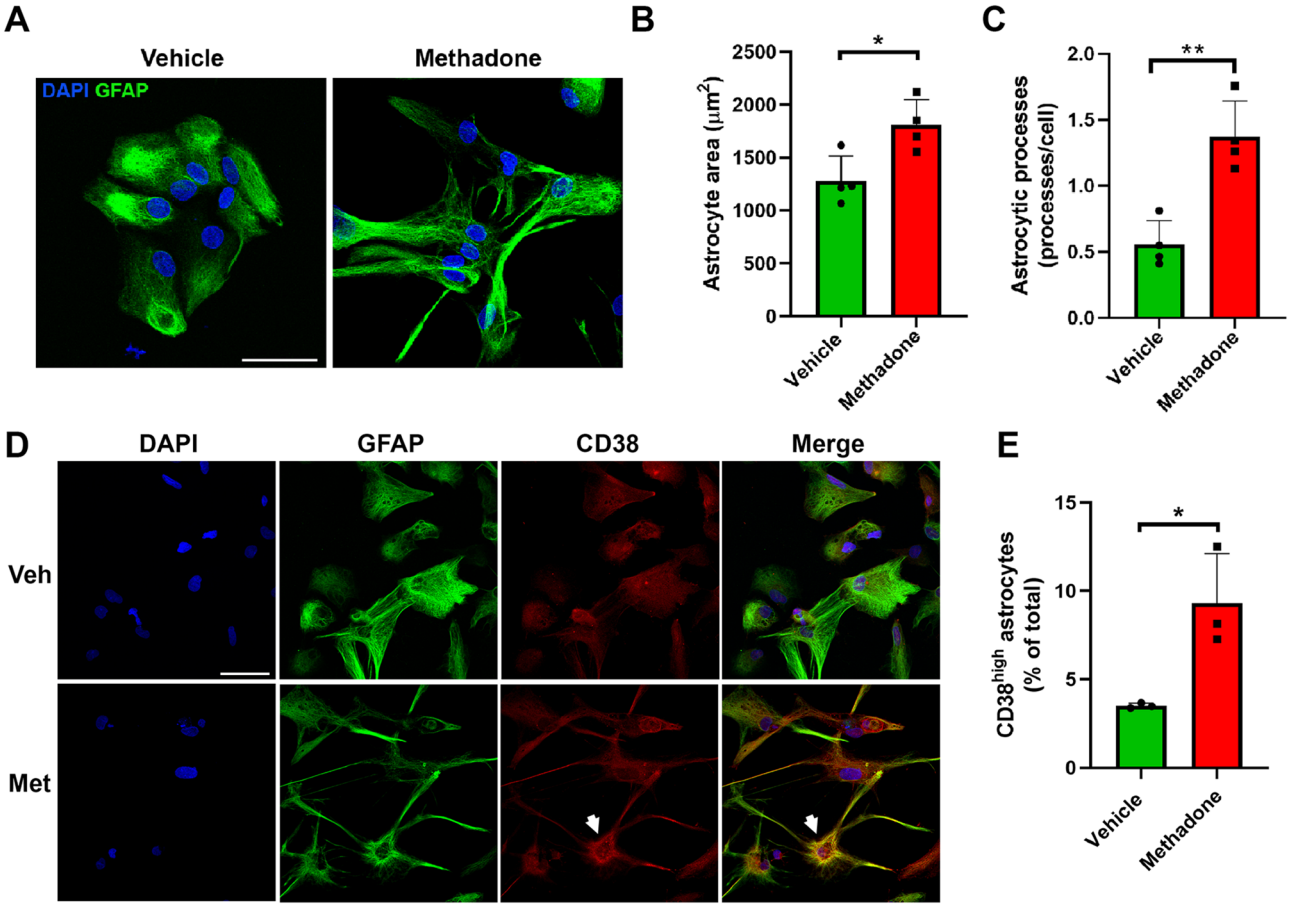

Figure 7. Chronic methadone treatment induces astrocyte activation. One-day-old primary astrocyte cultures were treated for three days with either 10 μM methadone or vehicle. (**A**) Representative confocal microscopy images showing astrocyte activation, evidenced by changes in cellular morphology visualized through the Glial Fibrillary Acidic Protein marker (GFAP, green). Nuclei were counterstained with DAPI (blue). Scale bar = 50 μm. (**B**–**C**) Quantification of the astrocyte area (**B**) and the mean number of astrocytic processes per cell (**C**). (**D**) Representative confocal microscopy images showing astrocyte activation evidenced by the expression of the activation-associated marker CD38 (red) in GFAP + cells (green). (**E**) Quantification of activated astrocytes based on increased levels of activation-associated marker ($CD38^{high}$), combined with a stellate $GFAP^{+}$ cell morphology. Data are presented as mean ± SEM of three independent cultures. In total, ~ 300 astrocytes were quantified for each condition. *$p < 0.05$; **$p < 0.01$ Student's T-test.

cytokine that promotes microglia homeostasis and resting state, preventing spontaneous activation and helping to reduce divergence between independent experiments[57–59]. For microglia, among the different cytokines evaluated we observed a significant ~ 3.5 fold increase in IL6 mRNA levels after a three-day methadone treatment (Fig. 8A). On the other hand, the three-day methadone treatment to astrocyte primary cultures failed to show significant alterations in proinflammatory mRNA analyses (Fig. 8B). However, due to the higher variability of primary cultures we also investigated proinflammatory alterations in microglia (HMC3) and astrocyte (DI TNC1) cell lines. Indeed, cell lines treated with the same three-day methadone scheme showed a significant increase in IL6, TNFa, and IL8 mRNA levels for HMC3 cells (Fig. 8C) and a significant increase in TNFa and CCL5 mRNA levels for DI TNC1 cells (Fig. 8D) compared to vehicle-treated cells. Taken together, these results show that methadone directly induces neuroinflammatory activation in isolated microglia and astrocyte cultures.

Methadone reduction of cell viability dependency on opioid receptors activation

To study whether the direct effect of methadone treatment on isolated neurons, oligodendrocytes, microglia, or astrocytes was dependent on opioid receptors, we examined whether the co-treatment of methadone with the opioid receptor antagonist naloxone for three days could prevent the reduction in cell viability induced by methadone. Results show that 100 μM naloxone did not significantly alter methadone-induced viability reduction at 10 μM or at the IC_{50} methadone concentrations, in any of the assayed cells (Fig. 9A–D), which suggests that methadone affected CNS cell viability via a non-canonical pathway.

Discussion

In this study, we examine for the first time the direct effects of methadone at therapeutically relevant concentrations on single brain cell types, all of which express opioid receptors in the developing CNS[60].

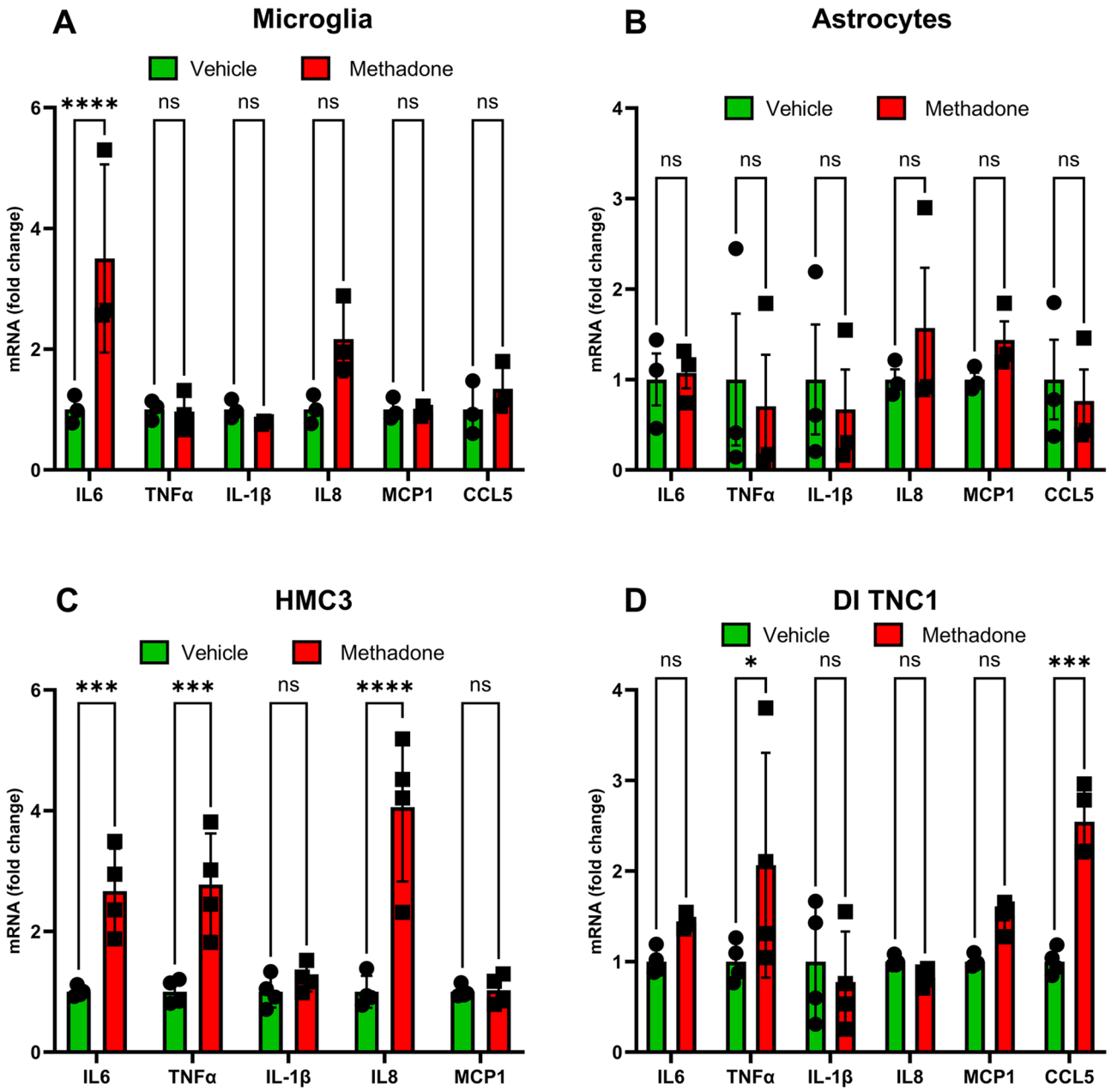

Figure 8. Chronic methadone treatment induces proinflammatory mRNA expression in cultured microglia and astrocytes. Primary microglia cultures, primary astrocyte cultures, HMC3 microglia cell line, and DI TNC1 astrocyte cell line were treated for three days with either 10 µM methadone or vehicle. Comparison of mRNA levels of proinflammatory cytokines in methadone-treated primary microglia (**A**), methadone-treated primary astrocytes (**B**), methadone-treated HMC3 microglia cell line (**C**), and methadone-treated DI TNC1 astrocyte cell line (**D**), compared to vehicle-treated controls. The expression levels of each target gene was normalized to the expression level of GAPDH in the same sample and expressed as fold change relative to the vehicle-treated controls. Data are presented as mean ± SEM of three (primary cells) to four (cell lines) independent cultures. *$p < 0.05$; **$p < 0.01$, ***$p < 0.001$ ****$p < 0.0001$ Two-way ANOVA with Šídák's multiple comparisons test.

It has been proposed that methadone-induced cognitive and behavioral alterations are associated with functional impairments of the main brain-resident cell types, including neurons, oligodendrocytes, microglia, and astrocytes[25,35,61–63]. In the brain, different cell types are in constant interaction with each other, and they receive blood-borne signals, e.g. from the peripheral immune system. Therefore, these alterations could be mediated by the direct effects of methadone acting on each individual cell type, but also indirectly by the action on selective cell types or by periphery-to brain signaling pathways. For instance, it has been reported that the production of proinflammatory cytokines by microglia and astrocytes impairs the differentiation of oligodendrocyte precursor cells and increase the apoptosis of mature oligodendrocytes, ultimately leading to decreased myelination[64–66]. Furthermore, the reduction of brain-derived neurotropic factor (BDNF) and insulin-like growth factor-1 (IGF-1)

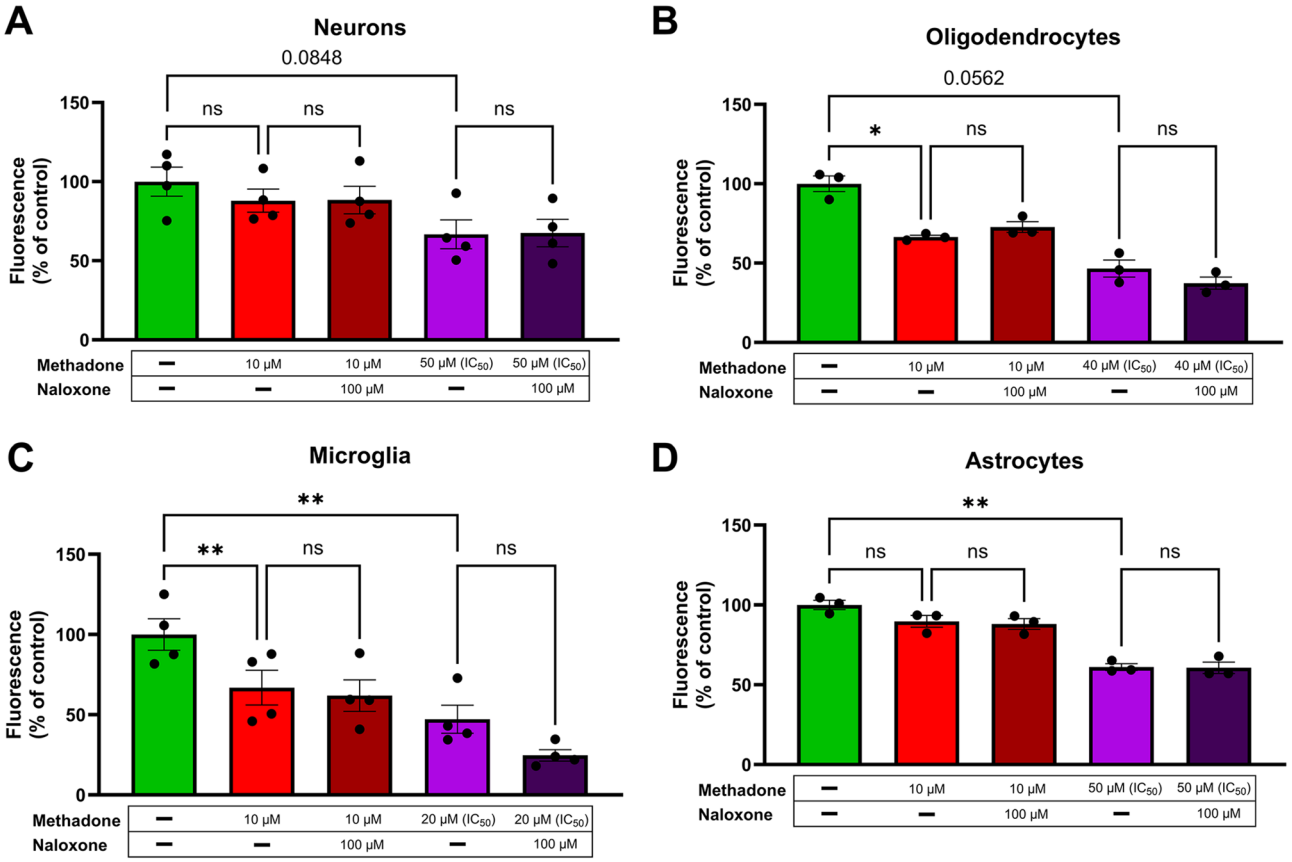

Figure 9. Naloxone co-treatment with methadone does not alter methadone-induced viability reduction in primary neuron, oligodendrocyte, astrocytes, or microglia cultures. Primary neuron (**A**), oligodendrocyte (**B**), microglia (**C**), or astrocyte (**D**) cultures were co-treated with to 10 μM or their corresponding IC_{50} methadone concentrations and 100 μM naloxone or vehicle, for three days. Cell viability was assessed using CellTiter-Blue analysis. Plots display the mean fluorescence normalized to vehicle-treated controls. Data are presented as mean ± SEM of 3–4 different biological replicates with 3 technical replicates each. *$p < 0.05$; **$p < 0.01$ One-way ANOVA with Tukey's multiple comparisons test.

levels, induced by opioid exposure, can negatively impact oligodendrocyte maturation and survival[67,68]. On the other hand, the proinflammatory mediators derived from microglia and astrocytes can directly impact neurons by initiating programmed cell death pathways[69,70], while oligodendrocyte alterations significantly contribute to axon damage and neuronal dysfunction[71]. Both neuronal and oligodendrocyte death has been linked to the impaired ability of activated astrocytes to promote neuronal survival, outgrowth, and synaptogenesis[72]. In addition, neurons cultured with activated astrocytes exhibited 50% less synapses compared to neurons grown with resting astrocytes[72].

Understanding the mechanisms through which methadone impacts fetal brain development is crucial for evaluating treatment options for OUD during pregnancy. This understanding can help to identify the specific targets of methadone that induce malaise and could potentially minimize adverse effects on the fetus. To achieve this goal, the generation and characterization of new models of greater simplicity are highly needed. In this context, Wu et al.[31]. has made significant advancements in studying the neural toxicity of methadone on cortical organoids. This model has been validated as a relevant neuron-glia 3D system for studying nervous system development under specific pharmacology treatments[31,35,36,73]. However, one drawback of this in vitro model is that organoids are generated from human induced pluripotent stem cells (hIPSCs), which may not consistently emulate the temporal development, cellular differentiation, and multicellular interactions observed during the intricate embryonic development of the mammalian brain. Additionally, it is not possible to dissect the independent effects that methadone might have on each neural cell type.

Other works conducted by Nylander et al. have investigated the toxic effects of various opioids, such as morphine, fentanyl, and methadone, on the viability of immortalized cell lines of neural origin[32] and in primary mixed cortical cell cultures from rats[30,74,75]. However, in these mixed cultures, cell type differentiation was not performed, making it impossible to analyze the specific toxicity effects of methadone on each specific cell type individually.

In this sense, primary cultures of the isolated different brain cell types emerge as a valuable tool for studying the direct effects of opioids on these cells. Here, we used highly pure primary cultures of neurons, oligodendrocytes, microglia and astrocytes obtained from E18 rat embryos or neonatal rats, which were incubated with

methadone for three days. However, whether our isolated cultures of these cells express opioid receptors needs to be further discussed. Transcriptome analyses of primary cultures of CNS cells show that their receptor pattern is not necessarily replicating what is observed in vivo[76]. In addition, it has been shown that the different strategies to obtain the cultures can alter their protein expression[77]. Therefore, we opted to include references of studies that show opioid receptor expression in cells obtained similarly to the present study. Historically, embryonic rat cortical neurons respond to specific opioid stimulation and antagonism, suggesting their functional expression of mu, delta, and kappa-opioid receptors[78,79]. Astrocytes obtained from P1-2 rat cortices show mRNA expression of mu, delta, and kappa-opioid receptors[80], respond to morphine and naloxone[81], and to delta and kappa-opioid receptor agonists[82]. Oligodendrocyte precursor cells obtained from newborn rat cerebral hemispheres express kappa and mu-opioid receptors for at least 30 days of culture[83]. It has also been shown that rat-derived primary microglia cells express mu-opioid receptors and show naloxone-dependent responses after exposure to an opioid agonist[84].

In concordance with the literature[75], we showed that the IC_{50} for methadone in neuron, oligodendrocyte, microglia, and astrocyte primary cultures ranges between 20 and 50 µM, which is higher than the methadone dose commonly detected in the plasma of pregnant women under opioid replacement therapy[27,28]. This suggest that therapeutically relevant methadone concentrations (2–10 µM) do not induce massive cell death in isolated primary cultures. Thus, we decided to incubate the different primary cell types with 10 µM methadone for three days to emulate opioid replacement therapy in vitro, a methadone treatment scheme also used in organoids and mixed cells culture studies[30,35]. We also showed that a naloxone co-treatment to neuron or glial cultures do not alter the viability impairment induced by methadone (either at 10 µM or at methadone IC_{50} concentrations for each cell type) at a naloxone concentration that has been previously reported to antagonize mu, delta, and kappa-opioid receptors[85]. This suggests that this direct toxic alteration of cell viability after a methadone treatment occurs via a non-opioid receptor pathway, such as its activation of acetylcholine receptors[86] or others, regardless of the brain cell exposed.

Studies in animals exposed to opioids in utero have demonstrated a decrease in the number of mature neurons in the cerebral cortex[87] and the hippocampus[33,34], areas of the brain associated with memory and learning. An effect that could be the result of insults secondary to methadone toxic effects. However, for the case of primary neurons, we observed that chronic methadone treatment induced a significant increase in cCaspase-3 levels, suggesting apoptosis induction.

Additionally, we observed a significant reduction in synaptic density in mature neurons, as evidenced by a decrease in colocalizing *puncta* and colocalizing area of the presynaptic and postsynaptic markers synaptophysin and PSD-95, respectively, consistent with a possible loss of synapses. These findings agree with prior studies that show that methadone impacts in vivo synaptic physiology[88], alters the composition of the pre- and postsynaptic components[36], and induces the suppression of neuronal function through altered electrophysiological properties[31] in cortical organoids. Further electrophysiological and electron microscopy studies are needed to confirm the direct effects of methadone over the synapse structure and function, and to dissect the specific molecular mechanisms associated to these impairments.

Oligodendrocytes, the myelin-producing cells in the CNS, are generated from highly proliferative progenitors that undergo several stages of differentiation before becoming mature myelinating cells[89]. This complex sequence of events is subjected to multiple regulatory mechanisms, making the generation of mature oligodendrocytes and myelin formation among the most vulnerable processes during brain development[90]. High-resolution magnetic resonance studies of infants with prenatal opioid exposure, including methadone, have demonstrated a significant decrease in fractional anisotropy,—a marker of axonal diameter and myelination—in brain regions responsible for impulsive control and motivation[91,92]. Myelin insulation, due to its essential role in the efficient conduction of brain impulses, has been directly associated with cognitive abilities, working memory, and anxiety responses[93]. Therefore, hypomyelination may underlie the increased risk of cognitive and behavioral difficulties commonly observed in children with prenatal opioid exposure. Accordingly, we observed that the incubation of primary oligodendrocyte cultures with 10 µM methadone for three days resulted in a significant increase in the apoptosis of pre-myelinating oligodendrocytes and impaired oligodendrocyte maturation. These data agree with previous reports in animal models of prenatal methadone exposure showing a significant increase in the apoptosis of myelinating oligodendrocytes and impaired differentiation of oligodendrocyte precursor cells[24,25], suggesting that the maturation process from OPCs to myelinating oligodendrocyte is disturbed by methadone exposure. OPCs express mu-opioid receptors during proliferation and maturation, then downregulate mu-opioid expression and develop kappa-opioid receptors once differentiated[83]. There is evidence supporting a crucial role of the endogenous opioid system in myelination[42], providing potential explanation for the direct effects of methadone on myelination. However, our oligodendrocyte isolation protocol resulted in a high proportion of differentiated pre-myelinating oligodendrocytes (> 95% of the total population). This limitation prevented us from assessing whether methadone could be involved in the apoptosis of OPCs and in the maturation step from OPCs ($NG2^+$ cells) to differentiated oligodendrocytes[41].

Interestingly, we observed that the co-incubation with the promyelinating hormones T3 and T4 leads to a three-fold increase in the MBP^+ population in methadone-treated oligodendrocytes, suggesting that methadone-induced impairments could potentially be reversed by stimulating alternative salvage pathways. This finding suggests that co-therapies accompanying opioid replacement therapy could be beneficial in normalizing the reduced myelination observed after methadone exposure. For instance, sobetirome, which mimics T3 thyroid hormone to promote OPC differentiation and myelin repair in short-term disease settings[94], may serve as a methadone co-therapy to induce remyelination in the CNS. Remyelination therapies, which target myelin disorders such as multiple sclerosis, may also be advantageous as co-therapies with methadone to counteract myelination impairment. In this sense, treatment with the kappa-opioid receptor agonist (±)U-50488 significantly enhances differentiation and myelination in purified oligodendrocyte cultures and greatly accelerates the kinetics of remyelination

in vivo[95]. Moreover, (±)U-50488 promotes the differentiation of hIPSCs-derived OPCs[95], suggesting that kappa-opioid receptor agonism is likely to be an effective strategy for remyelination in humans.

While acute opioid administration has been linked to immunosuppression[96], chronic opioid administration up-regulates pro-inflammatory cytokines at peripheral level[44,45], while at central level, it induces microglia and astrocyte activation, hallmarks of neuroinflammation[97]. Although, it was not reported whether microglia and astrocyte activation were secondary to the peripheral inflammation or directly produced by central opioid activity. In our study, we showed that in purified primary cultures of microglia and astrocytes, methadone incubation induced morphological and molecular changes indicative of proinflammatory activation, and also that primary microglia significantly increased the expression level of IL6. To overcome the more divergent nature of independent primary cultures that could mask changes, we also studied whether microglia or astrocyte cell lines increased their proinflammatory gene expression after the same three-day methadone treatment. We observed significantly increased levels of TNFα mRNA for both cell lines, IL6 and IL8 mRNA increases in the microglia cell line, and CCL5 mRNA increase in the astrocyte cell line, compared to the respective vehicle-treated cells. Non-classical methadone pharmacology may be responsible for this findings, as it directly activates the receptor for foreign molecules Toll-like receptor 4 (TLR4), triggering the activation of the NF-κB transcription factor[98], leading to the expression of proinflammatory molecules[46,47]. One limitation of the present study is the potential sex-differences in the responses induced by methadone incubation. Since neuronal cells were obtained at embryonic day 18 and microglia, astrocytes, and oligodendrocyte at post-natal day 0, unequivocal sex determination in these animals was difficult to perform. Nevertheless, each culture was obtained from the brains of four animals, likely containing male and female samples. Further studies could evaluate the direct methadone effect over cells obtained from male or female animals since emerging clinical data suggest sex-specific effects in infants including white matter injury following prenatal opioid exposure[99].

In this study, it has been determined that methadone independently and autonomously affects the four major cell types crucial for brain development. This work could serve as a starting point for studying, with greater resolution, the acute and chronic events that may be occurring in the neonatal brain in response to prenatal opioid exposure. The characterization performed in this study could be extrapolated to future morphological, functional, electrophysiological and pharmacological studies, which could subsequently be complemented with 2D and 3D co-culture studies to add greater complexity and achieve better resolution of both cell-autonomous and non-cell-autonomous specific mechanisms.

Conclusion

Opioid replacement therapy with methadone is the gold-standard treatment for pregnant women with OUD because it helps to reduce the return to illicit opioid use since treated pregnant women do not experience euphoria or withdrawal symptoms, promoting fetal stability. However, our data using highly purified developing brain cells indicated that chronic methadone exposure directly induces (i) neuronal apoptosis and a reduction in synaptic density; (ii) oligodendrocyte apoptosis and impaired myelination; and (iii) proinflammatory activation of microglia and astrocytes. In sum, the presented evidence suggest that therapies aimed to reduce the negative consequences of opioid substitution therapy would need to address a direct central effect of methadone on neurons, oligodendrocytes, microglia, and astrocytes, emphasizing the importance of finding new pharmacotherapies for maternal OUD.

Materials and methods

Animals

Generation of cortex-derived primary neuronal cultures

To obtain cortical neurons, pregnant Sprague Dawley rats were euthanized using a carbon dioxide (CO_2) chamber, in accordance with ARRIVE guidelines, and approved by the Universidad de los Andes Ethical Scientific Committee (Protocol CEC2022106). Following established procedures[100], rat embryos of 18 days (E18) were quickly removed and decapitated. Heads were placed on ice, and brains were collected in sterile cold phosphate buffered saline (PBS). For each culture, forebrain hemispheres were separated, meninges removed, and brain cortices of 4 embryos, likely containing male and female samples were isolated, collected in dissection media composed of 1X HBSS (Gibco) and 1 M HEPES buffer (Gibco), and digested with 0.25% trypsin (Gibco) for 15 min at 37 °C in a 5% CO_2 humidified incubator. Following digestion, tissues were washed three times with plating media, corresponding to Minimum Essential Medium (MEM, Gibco) supplemented with 10% horse serum (HS, Gibco), 1 mM sodium pyruvate (Gibco) and 0.6% w/v glucose (Sigma-Aldrich). Cortical tissue was triturated and dissociated using Pasteur pipettes. Finally, the cell suspension was seeded at a density of 75,000 cells/cm^2 on 96-well plates or 26,000 cells/cm^2 on 12 mm coverslips (pre-coated with 10 µg/mL poly-D-lysine, Gibco) in plating medium. After 3 h, the culture medium was removed, and neurons were maintained in Neurobasal Medium (Gibco) supplemented with 2% B27 (Gibco), 1X Glutamax (Gibco), 0.6% p/v glucose, penicillin–streptomycin (10,000 units/ml, Gibco), and 2.5 µg/mL amphotericin B (Corning) in a 5% CO_2 humidified incubator at 37 °C. The medium was replaced every 3 days.

Generation of cerebral cortex-derived primary glial cultures

To obtain the three main types of glial cells—microglia, oligodendrocytes, and astrocytes—we took advantage of their differential adherence properties. Mixed primary cultures of microglia, oligodendrocytes, and astrocytes were derived from the brain hemispheres of Wistar neonatal rats at post-natal day 0 (P0). All protocols were in accordance with ARRIVE guidelines, and approved by the Ethics Committee for experimentation with laboratory animals at the Medical Faculty, Universidad de Chile (Protocol CBA0943 FMUCH). After removing the meninges, the cortical tissue was collected from four pups, likely containing male and female samples. Tissue

was minced and enzymatically digested with 0.25% trypsin (Gibco) for 15 min at 37 °C. Then, tissue was treated with DNase I (Roche) at 60 µg/mL and mechanically disaggregated 20 times with a 5 mL serological pipette. Brain homogenate was allowed to decant, and after 5 min cell suspension was collected. This step was repeated once. The obtained cell suspension was centrifuged at 300 g for 15 min at room temperature. The cell pellet was resuspended in a medium composed of Dulbecco's Modified Eagle's Medium (DMEM, Gibco), supplemented with 10% fetal bovine serum (FBS, Hy-Clone), and 0.2% gentamicin (Sanderson), and evenly distributed among four T75 flasks. The culture medium was changed the following day and subsequently every 3 days.

After 12 days of culture, microglia were the first cell population purified from the primary mixed glial culture. The flasks were placed on an orbital shaker at 200 rpm for 1 h at 37 °C. The culture medium was collected and centrifuged at 600 g for 5 min, while fresh medium was added to the cells remaining in the culture flasks. The resulting pellet enriched in microglial cells was seeded at a density of 75,000 cells/cm^2 on 96-well plates, or 26,000 cells/cm^2 on 12 mm covers (pre-coated with 10 µg/mL poly-D-lysine) in DMEM supplemented with 1% FBS and 0.2% gentamicin. T75 flasks with fresh medium were mounted again on the orbital shaker for another 21 h at 200 rpm and 37 °C to separate oligodendrocytes from the remaining astrocyte layer. The cell suspension was collected and centrifuged at 600 g for 5 min. The resulting pellet containing oligodendrocytes was seeded at a density of 75,000 cells/cm^2 on 96-well plates or 26,000 cells/cm^2 on poly-D-lysine pre-treated coverslips in Neurobasal medium supplemented with 2% B27. After collecting microglia and oligodendrocytes, the astrocyte layer, that remains tightly adhered to the culture flask, was subjected to trypsinization. Cells were centrifuged at 600 g for 5 min and seeded at a density of 75,000 cells/cm^2 on 96-well plate or 26,000 cells/cm^2 on 12 mm covers in DMEM supplemented with 1% FBS and 0.2% gentamicin.

Evaluation of primary cell cultures purity by immunofluorescence

Primary cell cultures underwent two washes with phosphate buffered saline (PBS), followed by fixation using 4% paraformaldehyde (PFA, Merck) in PBS for 20 min at 37 °C. Subsequently, cells were washed three times with PBS, permeabilized with 0.2% Triton X-100 (Sigma-Aldrich) in PBS and blocked with 5% fish gelatin (Merck) for 1 h at room temperature. Cell samples were incubated with primary antibodies (Supplementary Table 1) at 4 °C overnight. Samples were washed four times with 0.1% Tween-20 (Sigma-Aldrich) in PBS and incubated with secondary antibodies (Supplementary Table 1) for 2 h at room temperature. Subsequently, they were washed four times with PBS. Nuclei were counterstained with DAPI (Sigma-Aldrich) and the samples were mounted with fluorescence mounting medium (Dako). Images were acquired in a Fluoview FV10i confocal microscope (Olympus), using Z-stack with 1 µm interval. 3D reconstruction (Z-stack) and image analysis were performed using Fiji software (NIH). To assess cell purity, positive cells for each lineage marker were counted relative to the total number of cells (DAPI$^+$ cells). At least 20 fields for each experimental condition were analyzed.

Determination of primary cell cultures viability after methadone treatment

Neurons, oligodendrocytes, microglia , and astrocytes were seeded at a density of 75,000 cells/cm^2 in 96-well plates, as described above. Cells were treated for three days with increasing concentrations of methadone ranging from 0.1 to 300 µM. The methadone treatment was renewed every 24 h. Cell viability was measured using the resazurin-based CellTiter-Blue assay (Promega). Hence, immediately after finalizing the methadone incubation, 20 µl of CellTiter-Blue reagent was added to each well according to the manufacturer's instructions. For neurons, astrocytes, and oligodendrocytes, the fluorescence was measured after 1.5-h incubation with CellTiter-Blue, using a microplate reader (Turner Biosystems) at excitation/emission wavelengths of 525/580–640 nm. Conversely, for microglia cultures, a 24-h incubation period with CellTiter-Blue was required to assess their viability due to a slower resazurin conversion.

Evaluation of neuronal apoptosis

To assess neuronal apoptosis, 6 days-old neuronal cultures were incubated in Neurobasal/2% B27 medium supplemented for three days with either 10 µM methadone or vehicle, with methadone renewal every 24 h. Neuronal apoptosis was evaluated measuring cleaved caspase-3 (cCaspase-3) by Western Blot and immunofluorescence. For Western Blot analysis, total proteins were extracted using RIPA buffer (Thermo-Fisher) containing protease inhibitors. 25 µg of proteins were used to examine the level of cCaspase-3 and total Caspase-3. The same membranes were assessed for β-actin immunoblotting as loading control (Supplementary Table 1). Reactive bands were detected using the Odyssey Imaging System (LI-COR) and quantified using the Image Studio Lite 5.2 software. For immunofluorescence evaluation, cell samples were double labeled with anti-cCaspase-3 antibody for detecting apoptotic cells, and anti-β-III tubulin as a neuronal marker (Supplementary Table 1). Images were captured in a Fluoview FV10i confocal microscope, and image analysis and Z-stack reconstruction were performed using Fiji software. Neuronal apoptotic cells were defined as cCaspase-3$^+$ and β-III tubulin$^+$ cells and were expressed as % of total neuronal population.

Evaluation of synaptic density in mature primary neurons

To assess synaptic density, 13-day-old neuronal cultures were incubated for three days in Neurobasal/2% B27 medium supplemented with either 10 µM methadone or vehicle, methadone was renewed every 24 h. After this period, neuronal cultures were fixed, permeabilized, and blocked as described above. Cell samples were incubated with PSD-95 (postsynaptic) and synaptophysin (presynaptic) antibodies (Supplementary Table 1) to determine the number of pre- and post-synaptic clusters by immunofluorescence. Images were captured using a Fluoview FV10i confocal microscope, and image analysis and Z-stack reconstruction were performed using Fiji software. Images were deconvolved with the software deconvolutionlab2 as previously reported[101]. Point spread function (PSF) was obtained from the confocal stacks of analyzed images for each fluorescent channel by using the FIJI

command "extract PSF". Then, the Richardson-Lucy algorithm was used to deconvolve images with 15 iterations for each channel of both synaptic proteins. A fixed region of interest (ROI) of all the dendrites proximal to the neuronal cell bodies were analyzed for each neuron. Only the most intense confocal slice (1 µm width) for both synaptic proteins was analyzed. From selected confocal slices, a binary mask to highlight synaptic puncta was independently stablished for both PSD-95 and Synaptophysin fluorescent channels. The average number of colocalizing PSD-95/Synaptophysin puncta was normalized by the corresponding ROI area. Finally, the average area covered by the overlapping pixels in each colocalizing puncta was quantified (PSD95/Synaptophysin colocalizing area).

Determination of apoptosis in oligodendrocytes

4-days-old oligodendrocytes cultures were incubated for three days in Neurobasal/2% B27 medium supplemented with either 10 µM methadone or vehicle, methadone was renewed every 24 h. After that period, oligodendrocyte cultures were fixed, permeabilized and blocked as described above. Cell samples were incubated with anti-cCaspase-3 antibody for detecting apoptotic cells (Supplementary Table 1). Images were captured in a Fluoview FV10i confocal microscope, and image analysis and Z-stack reconstruction were performed using Fiji software. Apoptotic oligodendrocytes were defined as cells positive for both cCaspase-3$^+$ and O4$^+$ (marker for differentiated oligodendrocytes[41]), and expressed as a percentage of total O4$^+$ cells. At least 20 fields for each experimental condition were analyzed.

Evaluation of oligodendrocyte myelination capacity

4-Days-old oligodendrocyte cultures were incubated for three days in Neurobasal/2% B27 medium (Gibco) supplemented with either 10 µM methadone or vehicle in the presence or absence of the thyroid hormones 3,3′,5-Triiodo-L-thyronine (T3, Sigma-Aldrich) and L-Thyroxine (T4, Santa Cruz Biotechnology) at a final concentrations of 20 ng/mL to promote oligodendrocyte myelination as described previously[43,102]. Methadone, T3 and T4 treatments were renewed every 24 h. After this period, oligodendrocyte cultures were fixed, permeabilized and blocked as described above. Cells were incubated with Myelin Basic Protein marker (MBP), a major component of the myelin sheath, and Oligodendrocyte Specific Protein (OSP), a specific oligodendrocyte marker (Supplementary Table 1). Images were captured using a Fluoview FV10i confocal microscope, and image analysis were performed using Fiji software. Myelinating oligodendrocytes were defined as MBP$^+$ and OSP$^+$ cells, and expressed as a percentage of the total oligodendrocyte population (OSP$^+$ cells). At least 20 fields for each experimental condition were analyzed.

Determination of microglia and astrocyte activation

One-day-old microglia and astrocyte cultures were incubated for three days in DMEM/1%FBS/0.2% gentamicin supplemented with either 10 µM methadone or vehicle, media that was renewed every 24 h. After that period, cells were fixed, permeabilized and blocked as described above. Cell samples were incubated with anti GFAP antibody as an astrocyte marker, with anti-CD38 antibody as astrocyte activation marker[56], and phalloidin for evaluating astrocyte morphology (Supplementary Table 1). Astrocyte cell area and the mean number of processes per cell (defined as a protrusion ≥ 20 µm-length) were quantified using Fiji software. Astrocyte activation was also evaluated by quantifying the number of CD38^{high} GFAP$^+$ astrocytes with an activated-like morphology (at least 1 protrusion ≥ 20 µm-length). For assessing microglia activation, microglia cultures were incubated with anti-CD11b and anti-CD45 antibodies. Iba-1 was used as a general microglia marker (Supplementary Table 1). Images were captured in a Fluoview FV10i confocal microscope, and image analysis and 3D reconstruction were performed using Fiji software. Activated microglia were defined as Iba-1$^+$ cells expressing high levels of CD11b or CD45 markers (CD11b^{high} or CD45^{high}), and amoeboid morphology as previously reported[48]. Cell population was determined as a percentage of total Iba-1$^+$. At least 20 fields for each experimental condition were analyzed.

Determination of mRNA levels of pro-inflammatory molecules by RT-qPCR

One-day-old microglia and astrocyte cultures were seeded in 12-well plates and incubated for three days in DMEM/1%FBS/0.2% gentamicin supplemented with either 10 µM methadone or vehicle, renewed every 24 h. Microglia media was also supplemented with M-CSF 20 ng/mL (Miltenyi) to prevent spontaneous activation. HMC3 (inmortalized human microglia, CRL-3304, ATCC) and DI TNC1 (inmortalized P1 rat astrocytes, CRL-2005, ATCC) cell lines were seeded at a density of 40.000 cells per well in 6-well plates to avoid overgrow and treated for three days using the same culture conditions as the primary cultures. Then, cells were washed and resuspended in 500 µL Trizol (Invitrogen). The aqueous layer containing the RNA was obtained by the addition of chloroform (Merck) and a 12,000×*g*, 15 min, 4 °C centrifugation, collected in new tubes, and 20 µg of molecular-grade glycogen (Invitrogen) was added to each sample. Then, the addition of isopropanol (Merck) and a 20-min incubation at − 20 °C was performed to promote RNA precipitation. Samples were centrifuged at 12,000×*g*, for 10 min at 4 °C, and an RNA pellet was obtained. Pellets were washed using 75% ethanol, resuspended in 12 µL RNAse/DNAse free water (Invitrogen), and stored at − 80 °C. One µg of RNA was used for the cDNA synthesis with M-MLV Reverse Transcriptase (Invitrogen). The expression levels of the proinflammatory molecules IL6, TNFa, IL-1β, IL8, MCP1 and CCL5 were determined by RT-qPCR using SYBR green (Brilliant II SYBR green master mix, Agilent) and QuantStudio 12K Flex (Thermo-Fisher) equipment. Data were normalized to the mRNA levels of glyceraldehyde-3-phosphate dehydrogenase (GAPDH). Primer sequences are listed in Supplementary Table 2.

Determination of the dependency of opioid receptors on methadone's effect on cell viability
Neurons, oligodendrocytes, microglia , and astrocytes were seeded as described above in 96-well plates. Cells were treated for three days with 10 μM methadone or the methadone concentration in which cell viability is inhibited by 50% (IC_{50}), obtained in previous three-day viability experiments, and co-treated with the opioid receptor antagonist naloxone at 100 μM or with vehicle. The media was renewed every 24 h. Cell viability was measured using CellTiter-Blue assay (Promega) as described above.

Statistical analysis
All experiments with primary cultures were conducted with three-to-four biological replicates (obtained from independent animals), unless otherwise indicated. When employing image analysis, the specific number of quantified cells was included in the corresponding figure caption. The normal distribution of data was verified using Shapiro–Wilk test. To assess the statistical significance of differences between two groups, a two-tailed Student's T-test was applied. For comparisons involving three or more groups, a one-way analysis of variance (ANOVA) followed by a Tukey post-hoc test was employed. For RT-qPCR analysis of expression of multiple genes, a two-way ANOVA was employed, followed by Šidák's multiple comparisons test. For non-parametric data Mann–Whitney test was used. For methadone dose response viability analyses, half-maximal inhibitory concentrations (IC_{50}) were determined by adjusting the data to a non-linear equation of methadone concentration (Log_{10}[Methadone]) vs. normalized response, using a variable slope model. P-values less than 0.05 were considered indicative of a significant difference. All statistical analyses were performed using GraphPad Prism V.9 software.

Data availability
All data supporting this study are included within the article and supporting material.

Received: 31 January 2024; Accepted: 16 July 2024
Published online: 23 July 2024

References
1. Kosten, T. R. & George, T. P. The neurobiology of opioid dependence: Implications for treatment. *Sci. Pract. Perspect.* **1**, 13–20. https://doi.org/10.1151/spp021113 (2002).
2. World Drug Report United Nations. https://www.unodc.org/unodc/data-and-646analysis/worlddrug-report-2022.html (2022).
3. Theisen, K. & Davies, B. J. The American opioid crisis: The inexorable march to death and addiction. *Eur. Urol.* **75**, 219–220. https://doi.org/10.1016/j.eururo.2018.10.051 (2019).
4. European Monitoring Centre for Drugs and Drug Addiction. https://www.emcdda.europa.eu/index_en2022 (2022).
5. St Marie, B., Coleman, L., Vignato, J. A., Arndt, S. & Segre, L. S. Use and misuse of opioid pain medications by pregnant and nonpregnant women. *Pain Manag. Nurs.* **21**, 90–93. https://doi.org/10.1016/j.pmn.2019.05.002 (2020).
6. Patrick, S. W., Davis, M. M., Lehman, C. U. & Cooper, W. O. Increasing incidence and geographic distribution of neonatal abstinence syndrome: United States 2009 to 2012. *J. Perinatol.* **35**, 667. https://doi.org/10.1038/jp.2015.63 (2015).
7. Smith, B. L. *et al.* Rates of substance and polysubstance use through universal maternal testing at the time of delivery. *J. Perinatol.* **42**, 1026–1031. https://doi.org/10.1038/s41372-022-01335-3 (2022).
8. Mattick, R. P., Breen, C., Kimber, J. & Davoli, M. Methadone maintenance therapy versus no opioid replacement therapy for opioid dependence. *Cochrane Database Syst. Rev.* https://doi.org/10.1002/14651858.CD002209 (2003).
9. Gynecologists, T. A. o. O. a. *ACOG Committee Opinion: Opioid Use and Opioid Use Disorder in Pregnancy* (2018).
10. Joseph, H., Stancliff, S. & Langrod, J. Methadone maintenance treatment (MMT): A review of historical and clinical issues. *Mt Sinai J. Med.* **67**, 347–364 (2000).
11. Women, A. C. o. H. C. f. U. & American Society of Addiction, M. ACOG Committee Opinion No. 524: Opioid abuse, dependence, and addiction in pregnancy. *Obstet. Gynecol.* **119**, 1070–1076. https://doi.org/10.1097/AOG.0b013e318256496e (2012).
12. Farid, W. O., Dunlop, S. A., Tait, R. J. & Hulse, G. K. The effects of maternally administered methadone, buprenorphine and naltrexone on offspring: Review of human and animal data. *Curr. Neuropharmacol.* **6**, 125–150. https://doi.org/10.2174/157015905908784533842 (2008).
13. Monnelly, V. J., Hamilton, R., Chappell, F. M., Mactier, H. & Boardman, J. P. Childhood neurodevelopment after prescription of maintenance methadone for opioid dependency in pregnancy: A systematic review and meta-analysis. *Dev. Med. Child Neurol.* **61**, 750–760. https://doi.org/10.1111/dmcn.14117 (2019).
14. Lee, S. J., Bora, S., Austin, N. C., Westerman, A. & Henderson, J. M. T. Neurodevelopmental outcomes of children born to opioid-dependent mothers: A systematic review and meta-analysis. *Acad. Pediatr.* **20**, 308–318. https://doi.org/10.1016/j.acap.2019.11.005 (2020).
15. Merhar, S. L. *et al.* White matter injury and structural anomalies in infants with prenatal opioid exposure. *Am. J. Neuroradiol.* **40**, 2161–2165. https://doi.org/10.3174/ajnr.A6282 (2019).
16. Levine, T. A., Davie-Gray, A., Kim, H. M., Lee, S. J. & Woodward, L. J. Prenatal methadone exposure and child developmental outcomes in 2-year-old children. *Dev. Med. Child Neurol.* **63**, 1114–1122. https://doi.org/10.1111/dmcn.14808 (2021).
17. Levine, T. A. & Woodward, L. J. Early inhibitory control and working memory abilities of children prenatally exposed to methadone. *Early Hum. Dev.* **116**, 68–75. https://doi.org/10.1016/j.earlhumdev.2017.11.010 (2018).
18. Nygaard, E. *et al.* Neuroanatomical characteristics of youths with prenatal opioid and poly-drug exposure. *Neurotoxicol. Teratol.* **68**, 13–26. https://doi.org/10.1016/j.ntt.2018.04.004 (2018).
19. Nygaard, E., Slinning, K., Moe, V. & Walhovd, K. B. Cognitive function of youths born to mothers with opioid and poly-substance abuse problems during pregnancy. *Child Neuropsychol.* **23**, 159–187. https://doi.org/10.1080/09297049.2015.1092509 (2017).
20. de Cubas, M. M. & Field, T. Children of methadone-dependent women: Developmental outcomes. *Am. J. Orthopsychiatry* **63**, 266–276. https://doi.org/10.1037/h0079429 (1993).
21. Kongstorp, M., Bogen, I. L., Stiris, T. & Andersen, J. M. Prenatal exposure to methadone or buprenorphine impairs cognitive performance in young adult rats. *Drug Alcohol. Depend.* **212**, 108008. https://doi.org/10.1016/j.drugalcdep.2020.108008 (2020).
22. Daly, F. M., Hughes, R. N. & Woodward, L. J. Subsequent anxiety-related behavior in rats exposed to low-dose methadone during gestation, lactation or both periods consecutively. *Pharmacol. Biochem. Behav.* **102**, 381–389. https://doi.org/10.1016/j.pbb.2012.05.010 (2012).
23. Lum, J. S. *et al.* Prenatal methadone exposure impairs adolescent cognition and GABAergic neurodevelopment in a novel rat model of maternal methadone treatment. *Prog. Neuropsychopharmacol. Biol. Psychiatry* **110**, 110281. https://doi.org/10.1016/j.pnpbp.2021.110281 (2021).

24. Gibson, J. M. *et al.* Perinatal methadone exposure attenuates myelination and induces oligodendrocyte apoptosis in neonatal rat brain. *Exp. Biol. Med.* **247**, 1067–1079. https://doi.org/10.1177/15353702221090457 (2022).
25. Jantzie, L. L. *et al.* Prenatal opioid exposure: The next neonatal neuroinflammatory disease. *Brain Behav. Immun.* **84**, 45–58. https://doi.org/10.1016/j.bbi.2019.11.007 (2020).
26. Vasan, V. *et al.* Neonatal opioid exposure: Public health crisis and novel neuroinflammatory disease. *Neural Regen. Res.* **16**, 430–432. https://doi.org/10.4103/1673-5374.293136 (2021).
27. Jansson, L. M. *et al.* Concentrations of methadone in breast milk and plasma in the immediate perinatal period. *J. Hum. Lact.* **23**, 184–190. https://doi.org/10.1177/0890334407300336 (2007).
28. Shiu, J. R. & Ensom, M. H. Dosing and monitoring of methadone in pregnancy: Literature review. *Can. J. Hosp. Pharm.* **65**, 380–386. https://doi.org/10.4212/cjhp.v65i5.1176 (2012).
29. Kongstorp, M., Bogen, I. L., Stiris, T. & Andersen, J. M. High accumulation of methadone compared with buprenorphine in fetal rat brain after maternal exposure. *J. Pharmacol. Exp. Ther.* **371**, 130–137. https://doi.org/10.1124/jpet.119.259531 (2019).
30. Nylander, E., Zelleroth, S., Nyberg, F., Gronbladh, A. & Hallberg, M. The protective and restorative effects of growth hormone and insulin-like growth factor-1 on methadone-induced toxicity in vitro. *Int. J. Mol. Sci.* https://doi.org/10.3390/ijms19113627 (2018).
31. Wu, W. *et al.* Methadone suppresses neuronal function and maturation in human cortical organoids. *Front. Neurosci.* **14**, 593248. https://doi.org/10.3389/fnins.2020.593248 (2020).
32. Nylander, E., Zelleroth, S., Nyberg, F., Gronbladh, A. & Hallberg, M. The effects of morphine, methadone, and fentanyl on mitochondria: A live cell imaging study. *Brain Res. Bull.* **171**, 126–134. https://doi.org/10.1016/j.brainresbull.2021.03.009 (2021).
33. Niu, L. *et al.* Impaired in vivo synaptic plasticity in dentate gyrus and spatial memory in juvenile rats induced by prenatal morphine exposure. *Hippocampus* **19**, 649–657. https://doi.org/10.1002/hipo.20540 (2009).
34. Golalipour, M. J., Ghafari, S., Kafshgiri, S. K., Moghadam, M. H. & Moharri, A. R. Effect of maternal morphine sulfate exposure on neuronal plasticity of dentate gyrus in Balb/c mice offspring. *Pak. J. Biol. Sci.* **16**, 281–286. https://doi.org/10.3923/pjbs.2013.281.286 (2013).
35. Yao, H. *et al.* Methadone interrupts neural growth and function in human cortical organoids. *Stem Cell Res.* **49**, 102065. https://doi.org/10.1016/j.scr.2020.102065 (2020).
36. Dwivedi, I. *et al.* Methadone alters transcriptional programs associated with synapse formation in human cortical organoids. *Transl. Psychiatry* **13**, 151. https://doi.org/10.1038/s41398-023-02397-3 (2023).
37. Robey, A., Buckingham-Howes, S., Salmeron, B. J., Black, M. M. & Riggins, T. Relations among prospective memory, cognitive abilities, and brain structure in adolescents who vary in prenatal drug exposure. *J. Exp. Child Psychol.* **127**, 144–162. https://doi.org/10.1016/j.jecp.2014.01.008 (2014).
38. Wu, M. *et al.* S100A8/A9 induces microglia activation and promotes the apoptosis of oligodendrocyte precursor cells by activating the NF-kappaB signaling pathway. *Brain Res. Bull.* **143**, 234–245. https://doi.org/10.1016/j.brainresbull.2018.09.014 (2018).
39. Li, Y. *et al.* Microglia activation triggers oligodendrocyte precursor cells apoptosis via HSP60. *Mol. Med. Rep.* **16**, 603–608. https://doi.org/10.3892/mmr.2017.6673 (2017).
40. Michalski, D., Keck, A. L., Grosche, J., Martens, H. & Hartig, W. Immunosignals of oligodendrocyte markers and myelin-associated proteins are critically affected after experimental stroke in wild-type and Alzheimer modeling mice of different ages. *Front. Cell Neurosci.* **12**, 23. https://doi.org/10.3389/fncel.2018.00023 (2018).
41. Nishiyama, A., Komitova, M., Suzuki, R. & Zhu, X. Polydendrocytes (NG2 cells): Multifunctional cells with lineage plasticity. *Nat. Rev. Neurosci.* **10**, 9–22. https://doi.org/10.1038/nrn2495 (2009).
42. Knapp, P. E., Maderspach, K. & Hauser, K. F. Endogenous opioid system in developing normal and jimpy oligodendrocytes: mu and kappa opioid receptors mediate differential mitogenic and growth responses. *Glia* **22**, 189–201. https://doi.org/10.1002/(sici)1098-1136(199802)22:2%3c189::aid-glia10%3e3.0.co;2-u (1998).
43. Emamnejad, R. *et al.* Thyroid hormone-dependent oligodendroglial cell lineage genomic and non-genomic signaling through integrin receptors. *Front. Pharmacol.* **13**, 934971. https://doi.org/10.3389/fphar.2022.934971 (2022).
44. Morcuende, A., Navarrete, F., Nieto, E., Manzanares, J. & Femenia, T. Inflammatory biomarkers in addictive disorders. *Biomolecules* https://doi.org/10.3390/biom11121824 (2021).
45. Newville, J., Maxwell, J. R., Kitase, Y., Robinson, S. & Jantzie, L. L. Perinatal opioid exposure primes the peripheral immune system toward hyperreactivity. *Front. Pediatr.* **8**, 272. https://doi.org/10.3389/fped.2020.00272 (2020).
46. Hutchinson, M. R. *et al.* Opioid-induced glial activation: Mechanisms of activation and implications for opioid analgesia, dependence, and reward. *Sci. World J.* **7**, 98–111. https://doi.org/10.1100/tsw.2007.230 (2007).
47. Wang, X. *et al.* Morphine activates neuroinflammation in a manner parallel to endotoxin. *Proc. Natl. Acad. Sci. USA* **109**, 6325–6330. https://doi.org/10.1073/pnas.1200130109 (2012).
48. Roy, A., Fung, Y. K., Liu, X. & Pahan, K. Up-regulation of microglial CD11b expression by nitric oxide. *J. Biol. Chem.* **281**, 14971–14980. https://doi.org/10.1074/jbc.M600236200 (2006).
49. Gao, C., Jiang, J., Tan, Y. & Chen, S. Microglia in neurodegenerative diseases: Mechanism and potential therapeutic targets. *Signal Transduct. Target Ther.* **8**, 359. https://doi.org/10.1038/s41392-023-01588-0 (2023).
50. Wendimu, M. Y. & Hooks, S. B. Microglia phenotypes in aging and neurodegenerative diseases. *Cells* https://doi.org/10.3390/cells11132091 (2022).
51. Brambilla, R. The contribution of astrocytes to the neuroinflammatory response in multiple sclerosis and experimental autoimmune encephalomyelitis. *Acta Neuropathol.* **137**, 757–783. https://doi.org/10.1007/s00401-019-01980-7 (2019).
52. Stiene-Martin, A., Gurwell, J. A. & Hauser, K. F. Morphine alters astrocyte growth in primary cultures of mouse glial cells: Evidence for a direct effect of opiates on neural maturation. *Brain Res. Dev. Brain Res.* **60**, 1–7. https://doi.org/10.1016/0165-3806(91)90149-d (1991).
53. Stiene-Martin, A. & Hauser, K. F. Opioid-dependent growth of glial cultures: Suppression of astrocyte DNA synthesis by met-enkephalin. *Life Sci.* **46**, 91–98. https://doi.org/10.1016/0024-3205(90)90041-o (1990).
54. Hauser, K. F. *et al.* mu-Opioid receptor-induced Ca^{2+} mobilization and astroglial development: morphine inhibits DNA synthesis and stimulates cellular hypertrophy through a Ca(2+)-dependent mechanism. *Brain Res.* **720**, 191–203. https://doi.org/10.1016/0006-8993(96)00103-5 (1996).
55. Patani, R., Hardingham, G. E. & Liddelow, S. A. Functional roles of reactive astrocytes in neuroinflammation and neurodegeneration. *Nat. Rev. Neurol.* **19**, 395–409. https://doi.org/10.1038/s41582-023-00822-1 (2023).
56. Roboon, J. *et al.* Deletion of CD38 suppresses glial activation and neuroinflammation in a mouse model of demyelination. *Front. Cell Neurosci.* **13**, 258. https://doi.org/10.3389/fncel.2019.00258 (2019).
57. Re, F. *et al.* Granulocyte-macrophage colony-stimulating factor induces an expression program in neonatal microglia that primes them for antigen presentation. *J. Immunol.* **169**, 2264–2273. https://doi.org/10.4049/jimmunol.169.5.2264 (2002).
58. Ponomarev, E. D., Novikova, M., Maresz, K., Shriver, L. P. & Dittel, B. N. Development of a culture system that supports adult microglial cell proliferation and maintenance in the resting state. *J. Immunol. Methods* **300**, 32–46. https://doi.org/10.1016/j.jim.2005.02.011 (2005).
59. Timmerman, R., Burm, S. M. & Bajramovic, J. J. An overview of in vitro methods to study microglia. *Front Cell Neurosci.* **12**, 242. https://doi.org/10.3389/fncel.2018.00242 (2018).

60. Hutchinson, M. R. *et al.* Exploring the neuroimmunopharmacology of opioids: An integrative review of mechanisms of central immune signaling and their implications for opioid analgesia. *Pharmacol. Rev.* **63**, 772–810. https://doi.org/10.1124/pr.110.004135 (2011).
61. Vestal-Laborde, A. A., Eschenroeder, A. C., Bigbee, J. W., Robinson, S. E. & Sato-Bigbee, C. The opioid system and brain development: Effects of methadone on the oligodendrocyte lineage and the early stages of myelination. *Dev. Neurosci.* **36**, 409–421. https://doi.org/10.1159/000365074 (2014).
62. Zamani, N., Osgoei, L. T., Aliaghaei, A., Zamani, N. & Hassanian-Moghaddam, H. Chronic exposure to methadone induces activated microglia and astrocyte and cell death in the cerebellum of adult male rats. *Metab. Brain Dis.* **38**, 323–338. https://doi.org/10.1007/s11011-022-01108-z (2023).
63. Navaei, F. *et al.* Chronic exposure to methadone impairs memory, induces microgliosis, astrogliosis and neuroinflammation in the hippocampus of adult male rats. *J. Chem. Neuroanat.* **125**, 102139. https://doi.org/10.1016/j.jchemneu.2022.102139 (2022).
64. Bonora, M. *et al.* Tumor necrosis factor-alpha impairs oligodendroglial differentiation through a mitochondria-dependent process. *Cell Death Differ.* **21**, 1198–1208. https://doi.org/10.1038/cdd.2014.35 (2014).
65. Shin, S. H., Kim, E. K., Lee, K. Y. & Kim, H. S. TNF-alpha antagonist attenuates systemic lipopolysaccharide-induced brain white matter injury in neonatal rats. *BMC Neurosci.* **20**, 45. https://doi.org/10.1186/s12868-019-0529-1 (2019).
66. Bonestroo, H. J., Heijnen, C. J., Groenendaal, F., van Bel, F. & Nijboer, C. H. Development of cerebral gray and white matter injury and cerebral inflammation over time after inflammatory perinatal asphyxia. *Dev. Neurosci.* **37**, 78–94. https://doi.org/10.1159/000368770 (2015).
67. Langhnoja, J., Buch, L. & Pillai, P. Potential role of NGF, BDNF, and their receptors in oligodendrocytes differentiation from neural stem cell: An in vitro study. *Cell Biol. Int.* **45**, 432–446. https://doi.org/10.1002/cbin.11500 (2021).
68. Ye, P., Carson, J. & D'Ercole, A. J. In vivo actions of insulin-like growth factor-I (IGF-I) on brain myelination: Studies of IGF-I and IGF binding protein-1 (IGFBP-1) transgenic mice. *J. Neurosci.* **15**, 7344–7356. https://doi.org/10.1523/JNEUROSCI.15-11-07344.1995 (1995).
69. McAdams, R. M. & Juul, S. E. The role of cytokines and inflammatory cells in perinatal brain injury. *Neurol. Res. Int.* **2012**, 561494. https://doi.org/10.1155/2012/561494 (2012).
70. Thornton, C. *et al.* Molecular mechanisms of neonatal brain injury. *Neurol. Res. Int.* **2012**, 506320. https://doi.org/10.1155/2012/506320 (2012).
71. Hayashi, Y., Jinnou, H., Sawamoto, K. & Hitoshi, S. Adult neurogenesis and its role in brain injury and psychiatric diseases. *J. Neurochem.* **147**, 584–594. https://doi.org/10.1111/jnc.14557 (2018).
72. Liddelow, S. A. *et al.* Neurotoxic reactive astrocytes are induced by activated microglia. *Nature* **541**, 481–487. https://doi.org/10.1038/nature21029 (2017).
73. Yao, H. *et al.* Buprenorphine and methadone differentially alter early brain development in human cortical organoids. *Neuropharmacology* **239**, 109683. https://doi.org/10.1016/j.neuropharm.2023.109683 (2023).
74. Gronbladh, A., Nylander, E., Zelleroth, S. & Hallberg, M. Assessing cell viability effects of opioids in primary cortical cells from rat. *Methods Mol. Biol.* **2201**, 171–180. https://doi.org/10.1007/978-1-0716-0884-5_15 (2021).
75. Nylander, E. *et al.* Growth hormone is protective against acute methadone-induced toxicity by modulating the NMDA receptor complex. *Neuroscience* **339**, 538–547. https://doi.org/10.1016/j.neuroscience.2016.10.019 (2016).
76. Cahoy, J. D. *et al.* A transcriptome database for astrocytes, neurons, and oligodendrocytes: A new resource for understanding brain development and function. *J. Neurosci.* **28**, 264–278. https://doi.org/10.1523/JNEUROSCI.4178-07.2008 (2008).
77. Freitag, K. *et al.* Diverse but unique astrocytic phenotypes during embryonic stem cell differentiation, culturing and development. *Commun. Biol.* **6**, 40. https://doi.org/10.1038/s42003-023-04410-3 (2023).
78. Vlaskovska, M. *et al.* Opioid effects on $45Ca^{2+}$ uptake and glutamate release in rat cerebral cortex in primary culture. *J. Neurochem.* **68**, 517–524. https://doi.org/10.1046/j.1471-4159.1997.68020517.x (1997).
79. Feng, Y. *et al.* Current research on opioid receptor function. *Curr. Drug Targets* **13**, 230–246. https://doi.org/10.2174/138945012799201612 (2012).
80. Ruzicka, B. B. *et al.* Primary astroglial cultures derived from several rat brain regions differentially express mu, delta and kappa opioid receptor mRNA. *Brain Res. Mol. Brain Res.* **34**, 209–220. https://doi.org/10.1016/0169-328x(95)00165-o (1995).
81. Kim, M. S. *et al.* Protective effects of morphine in peroxynitrite-induced apoptosis of primary rat neonatal astrocytes: Potential involvement of G protein and phosphatidylinositol 3-kinase (PI3 kinase). *Biochem. Pharmacol.* **61**, 779–786. https://doi.org/10.1016/s0006-2952(01)00541-x (2001).
82. Eriksson, P. S., Hansson, E. & Ronnback, L. Delta and kappa opiate receptors in primary astroglial cultures from rat cerebral cortex. *Neurochem. Res.* **15**, 1123–1126. https://doi.org/10.1007/BF01101714 (1990).
83. Tryoen-Toth, P., Gaveriaux-Ruff, C. & Labourdette, G. Down-regulation of mu-opioid receptor expression in rat oligodendrocytes during their development in vitro. *J. Neurosci. Res.* **60**, 10–20. https://doi.org/10.1002/(SICI)1097-4547(20000401)60:1%3c10::AID-JNR2%3e3.0.CO;2-O (2000).
84. Popiolek-Barczyk, K., Piotrowska, A., Makuch, W. & Mika, J. Biphalin, a dimeric enkephalin, alleviates LPS-induced activation in rat primary microglial cultures in opioid receptor-dependent and receptor-independent manners. *Neural Plast.* **2017**, 3829472. https://doi.org/10.1155/2017/3829472 (2017).
85. Wang, D., Sun, X. & Sadee, W. Different effects of opioid antagonists on mu-, delta-, and kappa-opioid receptors with and without agonist pretreatment. *J. Pharmacol. Exp. Ther.* **321**, 544–552. https://doi.org/10.1124/jpet.106.118810 (2007).
86. Pakkanen, J. S. *et al.* Methadone increases intracellular calcium in SH-SY5Y and SH-EP1-halpha7 cells by activating neuronal nicotinic acetylcholine receptors. *J. Neurochem.* **94**, 1329–1341. https://doi.org/10.1111/j.1471-4159.2005.03279.x (2005).
87. Wu, C. C. *et al.* Prenatal buprenorphine exposure decreases neurogenesis in rats. *Toxicol. Lett.* **225**, 92–101. https://doi.org/10.1016/j.toxlet.2013.12.001 (2014).
88. Slotkin, T. A., Whitmore, W. L., Salvaggio, M. & Seidler, F. J. Perinatal methadone addiction affects brain synaptic development of biogenic amine systems in the rat. *Life Sci.* **24**, 1223–1229. https://doi.org/10.1016/0024-3205(79)90059-6 (1979).
89. LeVine, S. M. & Goldman, J. E. Spatial and temporal patterns of oligodendrocyte differentiation in rat cerebrum and cerebellum. *J. Comp. Neurol.* **277**, 441–455. https://doi.org/10.1002/cne.902770309 (1988).
90. Mitew, S. *et al.* Mechanisms regulating the development of oligodendrocytes and central nervous system myelin. *Neuroscience* **276**, 29–47. https://doi.org/10.1016/j.neuroscience.2013.11.029 (2014).
91. Walhovd, K. B. *et al.* White matter characteristics and cognition in prenatally opiate- and polysubstance-exposed children: A diffusion tensor imaging study. *Am. J. Neuroradiol.* **31**, 894–900. https://doi.org/10.3174/ajnr.A1957 (2010).
92. Monnelly, V. J. *et al.* Prenatal methadone exposure is associated with altered neonatal brain development. *Neuroimage Clin.* **18**, 9–14. https://doi.org/10.1016/j.nicl.2017.12.033 (2018).
93. Nagy, Z., Westerberg, H. & Klingberg, T. Maturation of white matter is associated with the development of cognitive functions during childhood. *J. Cogn. Neurosci.* **16**, 1227–1233. https://doi.org/10.1162/0898929041920441 (2004).
94. Hartley, M. D. *et al.* Myelin repair stimulated by CNS-selective thyroid hormone action. *JCI Insight* https://doi.org/10.1172/jci.insight.126329 (2019).
95. Mei, F. *et al.* Identification of the Kappa-opioid receptor as a therapeutic target for oligodendrocyte remyelination. *J. Neurosci.* **36**, 7925–7935. https://doi.org/10.1523/JNEUROSCI.1493-16.2016 (2016).

96. Zhang, P. *et al.* Toll-like receptor 4 (TLR4)/opioid receptor pathway crosstalk and impact on opioid analgesia, immune function, and gastrointestinal motility. *Front. Immunol.* **11**, 1455. https://doi.org/10.3389/fimmu.2020.01455 (2020).
97. Garrido, E., Perez-Garcia, C., Alguacil, L. F. & Diez-Fernandez, C. The alpha2-adrenoceptor antagonist yohimbine reduces glial fibrillary acidic protein upregulation induced by chronic morphine administration. *Neurosci. Lett.* **383**, 141–144. https://doi.org/10.1016/j.neulet.2005.04.002 (2005).
98. Hutchinson, M. R. *et al.* Evidence that opioids may have toll-like receptor 4 and MD-2 effects. *Brain Behav. Immun.* **24**, 83–95. https://doi.org/10.1016/j.bbi.2009.08.004 (2010).
99. Madurai, N. K., Jantzie, L. L. & Yen, E. Sex differences in neonatal outcomes following prenatal opioid exposure. *Front. Pediatr.* **12**, 1357970. https://doi.org/10.3389/fped.2024.1357970 (2024).
100. Goslin, K., Asmussen, A. H., & Banker G. *Rat Hippocampal Neurons in Low-Density Culture. Culturing Nerve Cells, 2nd Edn* (1998).
101. Sage, D. *et al.* DeconvolutionLab2: An open-source software for deconvolution microscopy. *Methods* **115**, 28–41. https://doi.org/10.1016/j.ymeth.2016.12.015 (2017).
102. Miyamoto, Y. *et al.* Cdk5 regulates differentiation of oligodendrocyte precursor cells through the direct phosphorylation of paxillin. *J. Cell Sci.* **120**, 4355–4366. https://doi.org/10.1242/jcs.018218 (2007).

Acknowledgements

This work was supported by FONDECYT 1240162 and ACT210012 grants to Fernando Ezquer, FONDECYT 11240471 grant to Pablo Berríos-Cárcamo and FONDECYT 11220601 to Alejandro Luarte. Authors would like to thank Dr. Rene Vidal for sharing PSD-95 and synaptophysin antibodies. Additional support was provided by FONDEQUIP EQM190110 (QuantStudio 12K Flex Real-Time PCR System).

Author contributions

C de G; JG and PBC contributed equally to the study C de G: conception and design, collection of data, data analysis, manuscript writing, final approval of the manuscript. JG: conception and design, collection of data, data analysis, manuscript writing, final approval of the manuscript. PBC: conception and design, financial support, collection of data, data analysis, manuscript writing, final approval of the manuscript. AH: collection of data, final approval of the manuscript. DS: collection of data, final approval of the manuscript. AGM: collection of data, final approval of the manuscript ME: data analysis, final approval of the manuscript. PM: data analysis, final approval of the manuscript. AL: collection of data, data analysis, final approval of the manuscript. DC: collection of data, data analysis, final approval of the manuscript. UW: data analysis, final approval of the manuscript. FE: conception and design, financial support, data analysis, manuscript writing, final approval of the manuscript.

Competing interests

The authors declare no competing interests.

Additional information

Supplementary Information The online version contains supplementary material available at https://doi.org/10.1038/s41598-024-67860-7.

Correspondence and requests for materials should be addressed to F.E.